STAR CLUSTERS IN THEIR HOST GALAXY

Masters thesis by
Marcel Richard Haas

April 20, 2006

Masters thesis by Marcel Richard Haas, Utrecht University, April 2006

Supervisors:
prof. dr. Henny J.G.L.M. Lamers
drs. Mark Gieles

Universiteit Utrecht

Abstract

The work described in this thesis can be divided into two divisions, an investigation of the radii of star clusters in M51 and an investigation of the luminosity function of the population of clusters, or of subpopulations.

Reliable radius determinations are hard to make. The constraints on the data are severly reducing the sample, when investigating radii. Radii are determined by fitting a cluster profile convolved with the PSF of the optics, but this method is sensitive for contamination and highly varying backgrounds. The resulting radius distribution seems to be peaked at a value of around 3 pc, having a power law behaviour towards larger radii (similar to what is found in other studies). *Any relation between mean radius and postion in the galactic disk is not found, implying that the comparatively young cluster population is not in tidal equilibrium with their host galaxy (old globular clusters in our Milky Way halo are much closer to this equilibrium).*

The mass of the most massive cluster in a galaxy usually is determined by the cluster initial mass function (CIMF) and the star cluster formation rate (via the total number of clusters). *It is becoming clear, though, that there might exist a fundamental upper cluster mass limit, which in some galaxies* (among which M51) *is smaller than the limit implied by statistics.* I will show that the interacting galaxy M51 shows the signs of an upper mass limit, which varies with position in the disk. By comparing observed and simulated luminosity functions (LFs) of cluster populations I can infer the underlying CIMF. A physical upper mass limit for star clusters will appear as a bend in the LF, if the star cluster formation rate is high enough to sample the full range of cluster masses. The location of the bend in the LF provides information about the value of the upper mass limit. Using the LF of the star cluster population of M51 we show that the cluster initial mass function is likely to be truncated at the high mass end. *We also show that the maximum possible cluster mass in the central regions of the galaxy is higher than in the outskirts.* Regions of higher background intensity also tend to form more massive clusters.

Slopes of the luminosity function indicate a *more efficient cluster disruption process in the inner parts of the galaxy than in the outer parts, and more efficient disruption in high background regions than in regions with lower background intensity.*

Contents

Chapter 1

Introduction

The two main constituents of the universe are stars and gas (although mostly in the form of plasma). They do not exist separately from each other, ignoring their environment: they are continuously interacting. Stars are forming from gas and during their evolution they return chemically enriched gas and dust in the interstellar medium through winds and the explosions that mark the end of their lifes. From this enriched gas new generations of stars might form, with higher abundances of heavy elements.

1.1 Star formation in clusters

It is generally thought that the majority of stars (if not all of them) is born in star clusters (groups of several tens of stars to several million), see e.g. Larsen (2004). So, understanding the process of star formation is closely linked to understanding cluster formation and an explanation of the population of stars in a galaxy depends on the understanding of the birth and subsequent evolution of star clusters.

When one looks up at the sky on a clear night one sees just a few clusters and numerous loose stars, so-called 'field stars'. A simple, and correct, conclusion is that most stars do not live in clusters, but rather as single stars (except for the detail that most stars live in binary (or multiple) systems). This indicates that clusters are not very stable objects; if all stars are born in clusters, but most off them live alone, then most clusters must disrupt on rather short timescales.

1.2 Stellar population tracers

Star clusters consist of stars that are formed approximately coeval with all the same original composition. As a consequence of their compact nature, which makes them visible up to large distances, they are good tracers of the star formation history of their host galaxies. In contrast to the integrated light of a whole galaxy (which consists of an unknown mixture of stellar populations of different ages and metallicities), the integrated light of a single cluster gives, in a very simple way, information about the stellar population of the galaxy by comparison with simple stellar population models (SSP models), like the *GALEV* models (Schulz et al., 2002; Anders & Fritze-v. Alvensleben, 2003).

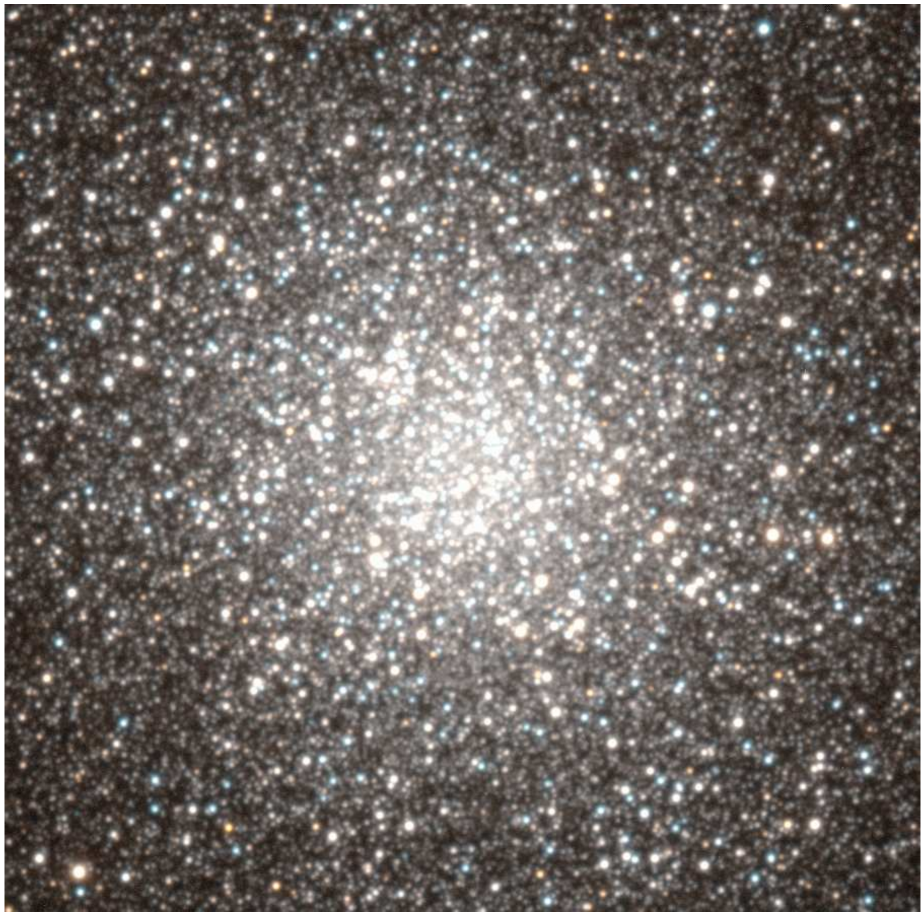

Figure 1.1:
In a halo around our Milky Way Galaxy, some 150 globular clusters like this (M22) are orbiting the galaxy. These objects usually are as old as the galaxy ($\pm$ 12 billion years) and show that some clusters might be able to survive for a long time. Image from http://crux.astr.ua.edu/gifimages/m22.gif

These SSP models and comparisons to clusters are on themselves important tests for stellar evolution models.

1.3 Cluster evolution

Besides their important implications for stellar as well as galactic evolution, star clusters are very interesting in their own right as well. Besides the already mentioned formation of clusters, also their dynamical evolution has many interesting aspects. Three very good books on this subject are Heggie & Hut (2003), Binney & Tremaine (1987) and Spitzer (1987).

The main interaction stars in a cluster have with each other is through gravity. Because of the nature of gravity a cluster is an intrinsically unstable object. A cluster in isolation will lose stars (mainly of low mass) by slow evaporation

Figure 1.2:
A typical example of a young cluster in our Milky Way: The Pleiades (M45). The gas that is left over after the formation of the stars is still present and visible. Removal of this gas might mark the end of the clusters lifetime. Image from http://fusionanomaly.net/pleiades.jpg.

(the high velocity tail of the their Maxwellian velocity distribution goes beyond the escape velocity) and by two- or more body interactions (giving the lower mass object a kick, such that it might escape; the higher mass counterpart will sink to the center of the cluster), see e.g. Spitzer (1987); Ostriker et al. (1972).

Things get even more complicated if the star formation was not 100% effective and gas is left over in the clusters, for example like in the Pleiades (Fig. 1.2). Removal of this gas by the stellar winds of masssive stars, or even by their supernova ejecta, makes the potential well of the cluster considerably less deep, resulting in a less bound cluster. See also Goodwin (1997); Geyer & Burkert (2001); Boily & Kroupa (2003); Fellhauer & Kroupa (2005); Melioli & de Gouveia dal Pino (2006).

This residual gas removal is the main cause of the 'infant mortality' of clusters. Most clusters do not survive the first 10 Myr of dynamical evolution (Lada & Lada (1991); Tremonti et al. (2001); Fall et al. (2005); Bastian et al. (2005b); Lamers et al. (2006) and references in the previous paragraph); they rather disrupt to form the galactic field star population.

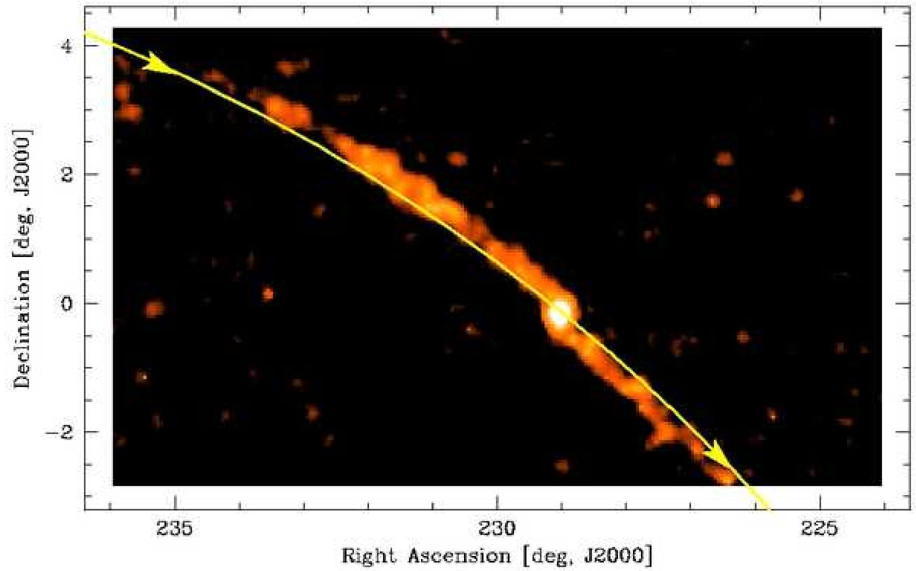

Figure 1.3:
Pal 5 is a good example of a cluster that is torn apart by the tidal field of our galaxy. One can clearly see two 'streams' of stars moving away on both sides of the cluster. The clusters orbit is indicated by the arrow. Stars closer to the galactic center are moving ahead, stars in the back of the cluster are lacking behind.

1.4 Clusters in interaction with their environment

Real clusters do not live in isolation. In the first place it feels the tidal field of its host galaxy. This makes sure that the cluster cannot grow as large as it would like, but it rather is tidally truncated. Stars outside its so-called tidal radius will be torn away by the tidal field of the galaxy, bringing these stars in another 'keplerian' orbit around the center of the galaxy, where they will have a different orbital period, cuasing the stars to lag behind or run in front of the cluster, moving further and further away. This can very clearly be seen in the case of Pal 5, Fig. 1.3. See Baumgardt & Makino (2003) for simulations of star clusters in tidal fields and Lamers et al. (2005) for an analytic description of the disruption of star clusters in tidal fields.

A second very important environmental aspect in cluster evolution is the interaction with other massive objects in the galaxy, like other clusters, Giant Molecular Clouds (GMCs) or the total gravitational well built up by all the material in a spiral arm. Everytime a cluster goes through a potential well its dynamics are drastically altered (Wielen (1991)). Moving towards the deepest part of the well the clusters is stretched, while it will get squeezed deep within it. Moving back out stretches the cluster again and a violent (close) encounter with a GMC or other cluster can strip a cluster for as much as 25% of its stars (Gieles et al., 2006d)!

1.5 Evolution and cluster parameters

We would like to quantify this incredibly complicated process of dynamical cluster evolution and eventually even come up with a complete prediction of the evolution of a cluster, once the initial parameters are known. Of course we are still very far from a definitive model, but important steps are already made. In particular the mass dependence of the disruption process is investigated in detail (theoretical, numericall as well as observational), see e.g. Baumgardt & Makino (2003); Boutloukos & Lamers (2003); Lamers et al. (2005). Dependencies on radius and the effect of the evolution on the luminosity function of the cluster population have had considerable less attention. These quantities will be the main topic of the present thesis.

1.6 Goal of research

In this research I will use a newly obtained set of observation of the interacting, face on, spiral galaxy M51, made with the Hubble Space Telescope, equipped with the Advanced Camera for Surveys. Because of the enormous field of view of the observations, together with the deepness and very high resolution we are able to search for relations between cluster parameters and their positions in the disk of M51. The observations allow us for the first time to study subpopulations within a galaxy without the loss of trustworthy statistics. I will focus on two main topics:

1. **Radii:** Is there a relation between the radius (distribution) of cluster(s) and their position in the disk (e.g. as a function of galactocentric distance or whether or not the cluster is in a spiral arm). This study will be published by Scheepmaker et al. (2006).

2. **Luminosities:** Is there a relation between the luminosity function of a cluster population and their position in the galaxy? This study will be published by Haas et al. (2006).

Of course, for both cases also explanations will be discussed.

This thesis is structured as follows. First, in Chapter 2 I will give a brief overview of the dynamics of star clusters (to create a framework for the observations) and I will describe photometric properties of a cluster (population). In Chapter 3 I will describe the data used in the investigation. Methods to obtain the results are described and discussed in Chapter 4, while the results themselves are given in Chapter 5 and 6. A concluding summary is given in the final Chapter (7).

In Appendix A I discuss statistical issues regarding the fitting of distribution functions in general, and power law distribution functions in special. Appendix B is reserved for a summary for non-astronomers.

Chapter 2

Star clusters and their evolution

This Chapter is devoted to giving a little theoretical background, in order to stand on firm grounds when analyzing the observations. Because of the topic of the thesis I will focus my attention to the radii and luminosities of clusters and what we will hope to be able to see.

2.1 Dynamical evolution

Studies to the dynamics of so-called 'N-body systems' go back as far as Einstein (1921). Pioneering in cluster dynamics he wrote a paper on M13, which was his only contact with clusters throughout his life. Although the conclusion he draws still holds (the non-luminous mass in the cluster contributes no higher order of magnitude to the cluster mass than does the luminous mass), considerable improvements in the field of cluster research have been made in due time. Whereas the earlier studies were oriented either observationally or analytically, with the development of computers the study of numerical dynamics became an important field of research as well. Special purpose hardware, like the *GRAPE* computers (Makino & Funato, 1993), make numerical integration of the dynamics of a star cluster even faster.

I will not treat the evolution of star clusters extensively, as that was not part of my project. Three very good books on cluster evolution and dynamics are Heggie & Hut (2003), Binney & Tremaine (1987) and Spitzer (1987).

In this section I will only summarize those dynamical aspects which have a visible influence or dependence on the radius.

2.1.1 Isolated star clusters

Although it is not really a relevant case for this study, isolated star clusters are a useful starting point to describe the evolution of a star cluster. The processes going on in an isolated cluster are after all not removed when the cluster interacts with its environment. Therefore I will briefly summarize it here; for details I refer to the beforementioned books.

For star cluster evolution, two time scales are particularly important: the crossing time (basically the size of the system divided by the typical stellar velocity) and the two-body relaxation time (the time in which the cumulative effect of two-body interactions can alter the stellar orbits significantly). See Henon (1973) for intuitive derivations.

The precollapse phase

The evolution of an isolated cluster is the slowest possible evolution sequence a cluster can undergo. Every process added to the evolution will speed up the evolution (usually leading to destruction). The first, long-lasting phase, is called the precollapse phase, because core collapse is what it eventually should lead to.

Two- or more-body interactions are of course a common phenomenon in dense stellar systems such as clusters. Whenever bodies interact, they tend to exchange energy in such a way that their energies get more equal (equipartition of energy). This comes down to the fact that that massive stars, on average, slow down and fall towards the center, whereas the less massive counterpart in the interaction will speed up to populate the outer regions of the cluster.

The interactions in a cluster will tend twoards a totally 'relaxed' state, one in which the velocity distribution is Maxwellian. Whenever stars get velocities in the fast tail of this distribution, they can be lost because their velocity exceeds the escape velocity of the clusters potential (another way of saying this is that the total energy of the star, potential (negative) plus kinetic, is positive). This *evaporation* of clusters make their potential well less deep, and therefore the escape velocity drops. If it were not for other processes, the cluster would disperse into field stars, leaving behind a small, very dense core.

Postcollapse evolution

Because of two-body interactions and the loss of stars from the outside the core gets denser and denser. Eventually this could lead to so-called core collapse. The formation of binaries, however, saves the cluster from such a disaster. Three-body interactions, in which one star takes enough energy to leave the remaining two in a bound state, or very close two-body interactions, in which by tidal effects the stars are slowed down, are able to form binaries. This formation of binaries releases energy and therefore the core starts to expand again. This will make sure that the core of the cluster survives the collapse.

The final fate of an isolated system of point masses

The processes described above do *not* take into account that clusters in reality consist of stars (except for the formation of a binary from tidal capture in a two-body interaction), rather than of point masses. In the, much simpler, case of a system of point masses the final state will be one of total dispersion. The stars will occupy an ever increasing volume, becoming less and less bound to what was once called the cluster.

2.1.2 Clusters in a tidal field

In reality a cluster is not on its own in the universe. Usually clusters belong to a galaxy, and are therefore influenced by their tidal field. Depending on the orbit of the cluster around the galactic center (circular or eccentric), the tidal field the cluster experiences can change strongly with time.

Using the tidal field of a galaxy it is not too hard to define a tidal radius, within which stars are bound to the cluster. Outside this radius, stars will generally be torn away from the cluster by the galaxy, in extreme cases leading to tidal tails on both side of the cluster like seen in Pal 5 (Fig. 1.3). Stars that are too close to the galactic center will be unbound from the cluster, reside in a closer Kepler orbit and therefore get a higher velocity and run ahead of the clusters. Stars that are too far of at the back end of the cluster will alse be torn away, lagging behind because of their lower Keplerian velocity. The tidal radius of a cluster with mass M at a galactocentric distance D_{gal}, with a Keplerian (circular) velocity V is given by

$$r_t = \left(\frac{GM}{2V^2}\right)^{1/3} \cdot D_{\mathrm{gal}}^{2/3} \tag{2.1}$$

Where G is the newtonian gravitational constant. If star clusters are in tidal equilibrium with their host galaxy it is to be expected that the radius of a cluster (or the mean/preferred radius of a cluster population) scales (with large scatter due to a scatter in mass) with the galactocentric radius.

The fact that star clusters are indeed in tidal equilibrium is used in many N-body simulations, like e.g. Baumgardt & Makino (2003). Cases like Pal 5 show that clusters sometimes are indeed as large as their tidal radius, but it remains to be seen whether this holds for any cluster, regardless of their position in the galaxy. Further out in the galaxy, tidal radii can get values of several tens of parsecs, which is unusually large for real clusters.

2.1.3 Clusters in interaction

Clusters do not 'live alone' in their host galaxy. They move in their orbits around the center together with many other clusters and Giant Molecular Clouds (GMCs). Clusters gravitationally interact with these other massive constituents. Also the movement through spiral arms (for disk clusters) or the movement through the disk (for halo clusters) strongly affects the dynamical state of a stellar system.

Disk and arm shocking

For this very concise summary I do not want to make a difference between shocking by a disk for halo clusters and shocking by a spiral arm for disk clusters. In both cases the star cluster moves through a region with a stronger gravitational potential due to a higher mass density. Whenever in this section 'arm' is mentioned, the same will hold for a disk.

Coming in the vicinity of the arm, the closest side of the cluster (as seen from the arm) will notice the effects of the potential well first. Stars at that side of the cluster will therefore be accelerated first and the cluster will be stretched. Inside the spiral arm, the effect will inverse: whereas the back end of the cluster still comes in at high speed (from the original acceleration) the front end stars are decelerated when climbing out if the potential well again. This squeezes the cluster in the same direction as it was originally stretched. When receding away from the spiral arm at the other end the cluster comes back in the old average galaxy potential. In the mean time, however, it could have lost a considerable amount of stars due to the stretching and squeezing (Wielen, 1991). A recent study to the effect of spiral arms on the dynamics of a cluster is done by Gieles et al. (2006a).

Encounters with other massive objects

Also the difference between encounters with other clusters and GMCs will be put equal here. The theory of cluster evolution under the influence of gravitational shocks is thoroughly discussed in Spitzer & Chevalier (1973).

Interactions with other massive objects, through their mutual attraction results in so-called 'heating' of the clusters. All stars get an acceleration in the direction of the other massive object. For all different stars in the cluster this is under a different angle with their original orbit around the cluster center. Continuing their orbit this therefore results in an increase in random velocities, making the cluster expand and becoming less bound. Very severe encounters can destroy a significant part of a cluster, as described by **?**.

2.1.4 Visibilty of dynamical state in the radius of a cluster

If one has a large sample of clusters at hand of which the determined (projected half light-) radii are reliable, we are able to see how well real clusters are described by numerical models. Of course it is not possible to follow the dynamical interaction of a single cluster in time, for the dynamical time scales are too long. We can, however, look for statistical correlations between cluster radii and their position with respect to their host galaxy or neighbouring clusters or GMCs.

If for example the majority of clusters is in tidal equilibrium with the galaxy, and the distribution of cluster radii has a certain peak, then it can be expected that this peak lies at larger radii for larger galactocentric distances (assuming that there indeed is no mass radius relation, like found by Bastian et al. (2005b)). If, on the other hand, the clusters are not at all confined by the tidal radius, but rather are much smaller, one does not expect a relation between preferred radius (peak of the distribution) and galactocentric distance.

The same reasoning holds for radius distributions in-/outside spiral arms and close to, or far from, massive objects.

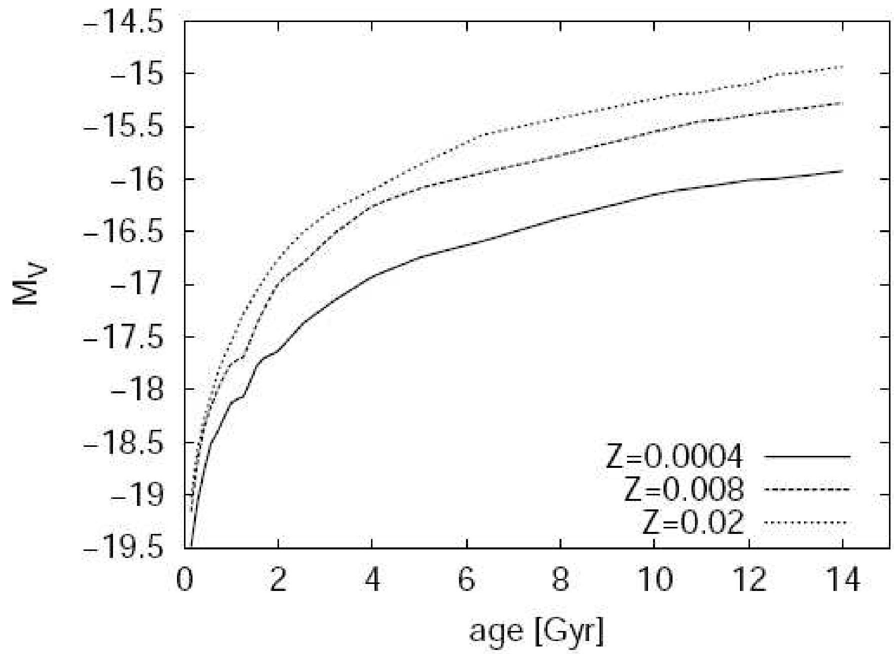

Figure 2.1:
The photometric evolution of a star cluster with a Salpeter IMF at the indicated metallicities. Different masses will only vertically shift the plots. Dynamical evolution is not taken into account (no loss of stars). The cluster fades due to stellar evolution only. Taken from Schulz et al. (2002).

2.2 The photometric properties of clusters

Besides the radius of a cluster, which will turn out to be hard to determine with great accuracy, we can investigate the photometric properties of a star cluster population in order to obtain results regarding their age, mass and/or extinction. This comes along with several uncertainties as described by de Grijs et al. (2005).

Extragalactic star cluster are too small to resolve their constituents stars (except, maybe, for some bright O or B stars). We therefore see the cluster as a (near) point source having a spectral energy distribution (SED) that consists of the sum of the SEDs of all its stars.

2.2.1 Photometric evolution of a cluster

Cluster are so-called 'simple stellar populations (SSPs)', meaning that they consist of stars with all the same age and the same original composition. Whereas ages and metallicity might differ slightly in a cluster, this generally is a very good approximation (except for exotic objects like Ω Cen, having three recognizable populations and is probably the result of the merger of several smaller clusters, see Sollima et al. (2005) and references therein).

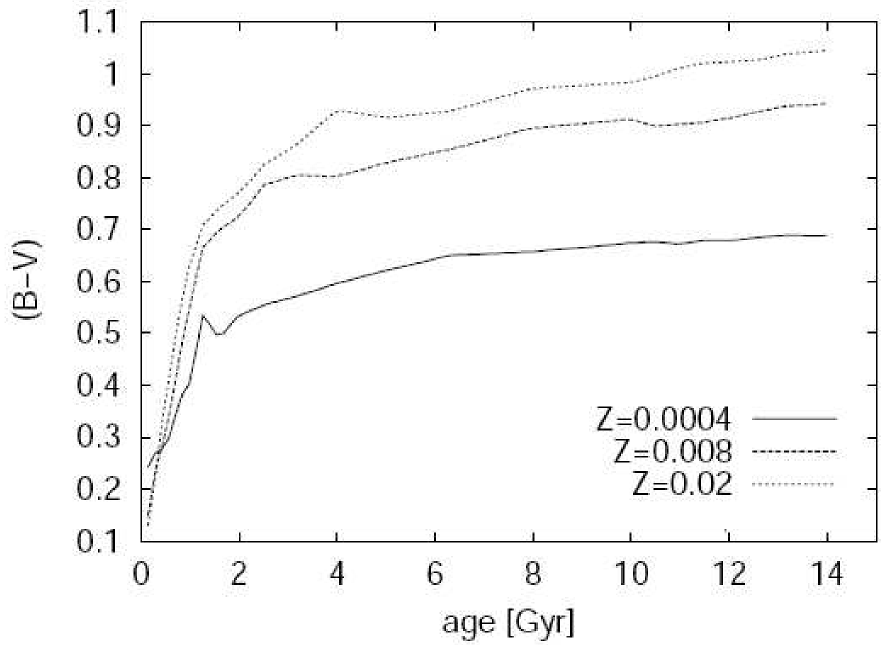

Figure 2.2:
The color evolution in Johnson $B - V$ for clusters of different metallicities, with a Salpeter IMF. Note that the color of a cluster does not depend on its mass. Dynamical evolution is not taken into account (no loss of stars), this is the result of stellar evolution only. Taken from Schulz et al. (2002).

Modelling photometry of star clusters can be done using a library of stellar spectra (either calculated from stellar evolution models or observationally obtained) of different stellar masses and metallicties. Well known examples of SSP models are the *GALEV* models (Schulz et al., 2002; Anders & Fritze-v. Alvensleben, 2003), which make use of the Padova evolutionary tracks (Bertelli et al., 1994; Girardi et al., 2000). These SSP models can give, for example, the time evolution of the absolute magnitude in a certain passband, or the color, as shown in Figs. 2.1 and 2.2. Of course this is dependent on the metallicity as well as the stellar IMF. These SSP models in general do not take into account the dynamical evolution of a cluster. All stars remain in the cluster (although they end up as dark remnant, contributing hardly to the photometry of the cluster). In order to model cluster photometry *including* dynamical evolution one has to jump in every time step to a star cluster of lower mass (just shifting the photometric evolution line to higher magnitudes) and possibly another stellar mass function (if you want to take into account that clusters preferentially loose low mass stars).

Determination of star cluster properties from photometry

If one only has access to photometry in several broad passbands, obtaining detailed information about a star cluster (like its mass, age, metallicity and

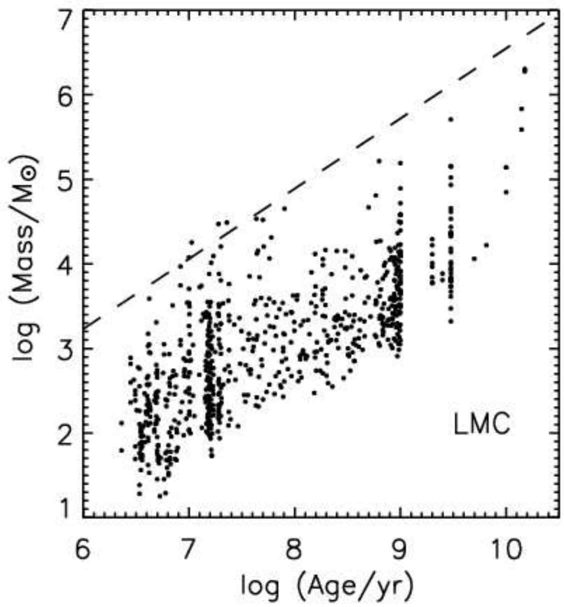

Figure 2.3:
Log(age/yr) plotted against log(mass/$M_{\odot}$) for the cluster population of the LMC, according to Hunter et al. (2003). The detection limit goes to higher masses for older clusters because clusters fade as they age. The shown dotted line is the expected increase of the maximum cluster mass at a certain age due to the size of sample effect (for a cluster population with constant formation rate and power law mass function with slope -2). Plot taken from Gieles et al. (2006b).

extinction) is hard. The main reason is a degeneracy: stellar evolution makes a cluster redder, but so does extinction and even a higher metallicity will work in the same way. It therefore is important to cover a large part of the SED, in order to obtain this information, like described in e.g. Bik et al. (2003); de Grijs et al. (2003a,b,c).

Our dataset will only contain B, V, I and Hα. This is not enough to obtain accurate masses, extinctions, ages and metallicities. We will have to use different techniques here and rather study the population as a whole, without taking care of all clusters separately.

2.2.2 Luminosity functions

A very useful tool in the study of star cluster populations is their luminosity function (LF). The LF is built up from clusters of all different ages, masses, metallicities and so on.

As an example of the use of a LF I will shortly explain the models described in Gieles et al. (2006b), using cluster data of the LMC from Hunter et al. (2003). In Fig. 2.3 the age is plotted against mass (both logarithmically). If all the age bins are equally sized in logarithmic space, then bins for older clusters should contain

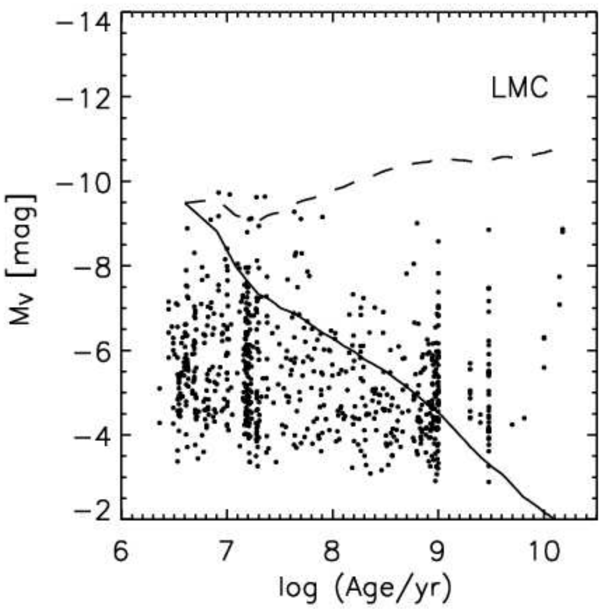

Figure 2.4:
The same clusters as in Fig. 2.3, but now with the absolute visual magnitude on the vertical axis. The detection limit now of course stays horizontally. The upper dashed line is the expected absolute magnitude of the most massive cluster, according to the size of sample effect. The solid line is the the evolutionary track of the most massive cluster in the first bin. Plot taken from Gieles et al. (2006b).

more clusters, because they correspond to a larger time interval. If the mass of a newly born cluster in the process of cluster formation is determined by statistics (masses according to a power law mass function $N(M)\mathrm{d}M \propto M^{-\beta}\mathrm{d}M$), then the mass of the most massive cluster is determined by the size of the sample and therefore going up in Fig. 2.3.

If we now plot the absolute magnitude of these clusters (which is a function of mass, age and metallicity) instead of the mass we obtain Fig. 2.4. Here we can see that the size of sample effect and the fading of clusters due to stellar evolution makes sure that the maximum luminosity of star clusters is more or less constant (the growing size of sample, and therefore mass of the most massive cluster, and the fading of clusters due to stellar evolution almost cancel each other out). This would also imply that the maximum cluster luminosity in a galaxy scales with the number of clusters in the galaxy and this is indeed what is found by Whitmore (2003) and Larsen (2002).

Obtaining a LF of the total star cluster population of a galaxy now, is nothing else than integrating this figure (2.4) in the horizontal direction, to see how many clusters there are in each magnitude bin. The fact that fading and the size of sample effect cancel each other out is the reason that the slope of the LF represents the slope of the cluster initial mass function (although they are not exactly the same).

An important conclusion is that exact measurements of cluster masses and ages are *not* required if one wants information about the CIMF. This is the reason several authors intensively investigated LFs of cluster populations in different galaxies and different environments. They all find a power law distribution function:

$$N(L)\mathrm{d}L \propto L^{-\alpha}\mathrm{d}L \tag{2.2}$$

with the exponent (α) between 1.8 and 2.4, see e.g. Larsen (2002); de Grijs et al. (2003a). This suggests that in most galaxies the CIMF will also be approximately a power law with an exponent of around -2.

2.2.3 An upper mass limit for clusters and the LF

It has to be noted that the power law LFs are only found for galaxies with young cluster populations. Old cluster populations (like the globular cluster population in our own Milky Way Galaxy) usually show log-normal distribution functions of their luminosities (Harris, 2001; Richtler, 2003). Nevertheless, these clusters also have a log-normal distribution of masses, so again the shape of the LF resembles the shape of the mass function.

In only three galaxies the LF of the star clusters is found to be better described by a double power law, i.e. two distinct parts, both described by a power law, which are seperated by a bend at certain absolute magnitude, which differs from galaxy to galaxy. Whitmore et al. (1999) found for the "Antennae" (NGC 4038/4039) a bend at $M_V \simeq -10$, with on the faint side a shallower slope (~ -2) than on the bright side (~ -2.7). For M51, Bastian et al. (2005b) found hints for a double power law, which were confirmed by Gieles et al. (2006c). The slopes on both sides are similar to the slopes found by Whitmore et al. (1999), but the bend occurs about 1.6 magnitude fainter. In Gieles et al. (2006b) it is shown that NGC 6946 is also better fit with a double power law, with parameters comparable to M51. *Note that the slopes at the faint end of the LF for all these galaxies are similar to the slopes found for populations with a single power law distribution.*

Whereas the bend in the LF of the "Antennae" was interpreted as a bend in the mass function by Whitmore et al. (1999), Gieles et al. (2006b) have shown with analytic cluster population models that such a bend can occur if the maximum possible cluster mass is not longer determined by the size of sample effect (as *is* the case for e.g. the LMC and SMC (Hunter et al., 2003), and is argued to be generally true by Weidner et al. (2004), who claim that the maximum cluster mass is a function of the star formation rate only), but that there rather exists a *physical upper mass limit* for star clusters. All the details of the explanation can be found in Gieles et al. (2006b), but I will shortly summarize the main features here. The model also corrects for dynamical effects, but I will leave that out of the discussion here, to maintain simplicity,

Let us assume that there exists a certain upper mass limit (or an exponential cut-off at the high mass end), see also Fig. 2.5. We again make a plot like Fig. 2.4, now analytically filled with clusters, with masses randomly sampled from a power law distribution function. If the star formation rate is high enough to sample *just* the whole range of possible cluster masses (i.e. the maximum mass in the youngest age bin due to the size of sample effect is equal to the physical upper mass limit), then the first age bin is precisely filled. The rest of

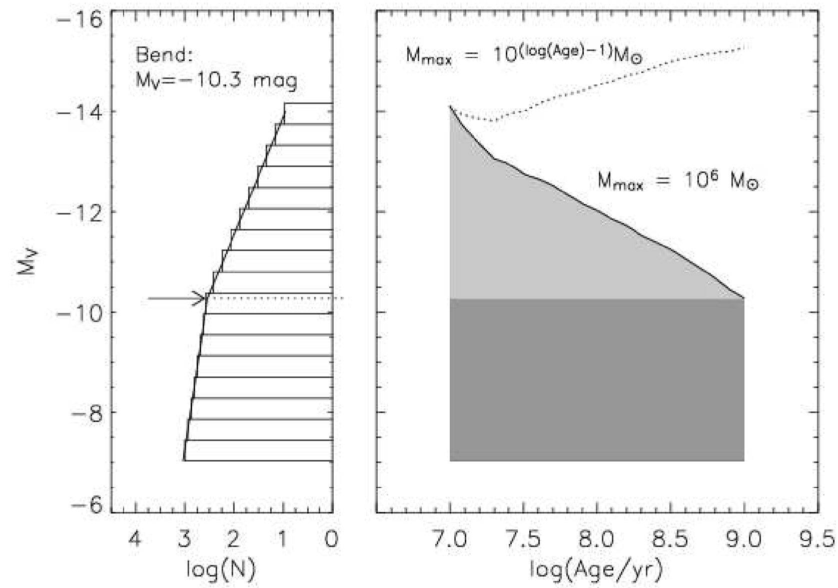

Figure 2.5:
The construction of a LF of a cluster population with an upper limit for the cluster mass. In the righthand panel you see a model for the plot as Fig. 2.4, with a truncation at the high mass end. The solid line now gives the maximum possible cluster luminosity per age bin, as the most massive cluster fades. Integration along lines of equal luminosity again gives the LF. For the dark shaded region, the slope is not different from before (although there are more clusters, if the cluster formation rate does not change). From the locatiopn of the oldest most massive cluster along the LF on towards the brighter end the LF will become steeper than without mass truncation. Plot taken from Gieles et al. (2006b).

the age bins should contain *more* clusters due to the larger sizes of the bins, but the mass of the most massive cluster cannot be more massive than the physical upper limit. This means that there *are* indeed more clusters, but that the solid line in Fig. 2.4 can be used here as describing the photometric evolution of the most massive (and therefore most luminous) cluster per age bin.

If, again, the LF is created by integrating horizontally, one can easily see that in the dark shaded region the situation is like the older situation: the shape of the LF is the same; the fact that there *are* more clusters with those luminosities (the total number is determined by the formation rate, and the distribution function cannot be sampled due to the physical upper limit, so there are *more* clusters with lower luminosities) does not change the shape of the LF, because a power law is scale free. Above this region, though, there are too little objects (an effect that is becoming stronger for higher luminosities), as indicated by the light shaded region. The integration therefore will result in an LF which is, on the faint side of the bend, the same as it would be without upper mass limit, but on the bright side it will be *steeper*.

If the formation rate of cluster is such that for the first few age bins the size of sample effect is still the most important constraining factor for the maximum mass in a bin, and only for the older bins the mass truncation is noticable, then the effect will be similar, but less clear. If, on the other hand, the formation rate is already sufficiently high to make the physical upper mass limit determine the maximum mass in the youngest age bin, the effect will be maximal, and one will obtain even a truncated LF. This LF will also show a bend at the luminosity of the oldest most massive cluster.

M51 is an interacting galaxy, with triggered star formation. The star formation rate is therefore expected to be reasonably high, so *if* there exists a maximum possible mass for clusters in M51, we might well detect a bend in the LF. Owing to the huge sample that will be described in Chapter 4, extracted from the data set described in the next Chapter (3) we can even try to look for variations across the disk of the galaxy.

Chapter 3

Observations of M51

In order to investigate the distribution of the radii and luminosities of star clusters and the dependencies on their position in their host galaxy we make use of a set of observations from the Hubble Space Telescope (HST), equipped with the Advanced Camera for Surveys (ACS).

There are several reasons why we would want to use the HST for this particular purposes, as mentioned by Larsen (2004). There are three main reasons. A first might be the superb angular resolution (0".05 for the ACS), which makes it able to resolve small clusters (radii of about 2-4 pc) out to distances up to 20 Mpc. A second one is the large field of view of eg. the ACS. With 200"x200" (both chips together) the field of view covers a significant fraction of a galaxy in a single pointing for galaxies not too far away. And the last, but certainly not least, reason is the spectral range the HST offers us. For a thourough investigation of young stellar populations, coverage of the whole spectral range from the near-UV to the near-IR is needed. For these reasons a lot of research to stellar populations of different ages is already carried out using HST; this is reviewed by Larsen (2004); Whitmore (2003).

The reason to use the particular dataset described below is easily explained. Never before there was such a huge part of a face-on galaxy imaged with this angular resolution and photometric deepness. Earlier M51 studies were limited to WFPC2 and NICMOS pointings, which did not cover the whole system, see e.g. Bik et al. (2003); Bastian et al. (2005b); Gieles et al. (2005); Lee et al. (2005). This new, total coverage of the whole system is a unique opportunity to investigate in great detail the whole population of clusters. Because of the recent interaction with NGC 5195 (Salo & Laurikainen (2000)), lots of young star clusters are present. A clear rise in cluster formation rate 50-70 Myr ago is confirmed by Bik et al. (2003). The large contrast between spiral arms and interarm regions is the last ingredient for a very useful set of data to investigate a large cluster sample and relations between cluster properties and the location in their host galaxy.

To celebrate Hubble's 15th anniversary, Cycle 14 HST proposers were encouraged to submit proposals to complement or analyze the unique dataset of M51. The images were taken as a part of the Hubble Heritage Project and became publicly available in April 2005.

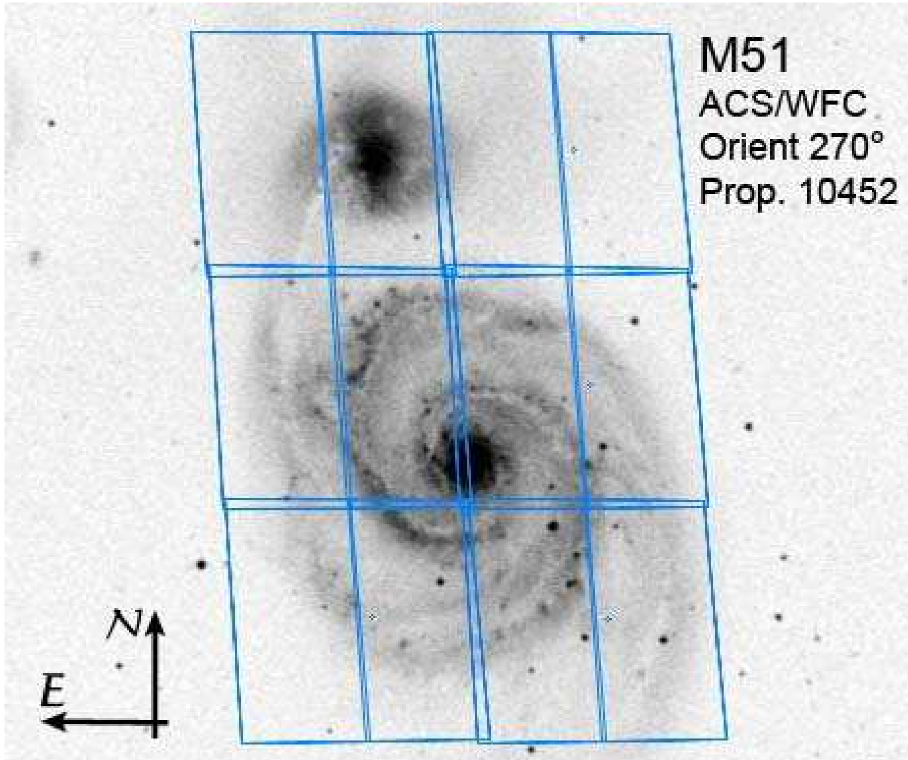

Figure 3.1:
On overlay of the six HST/ACS pointings that together make up the mosaic covering the whole system of M51, including companion (NGC 5194/5195) on a DSS image. All visible panels consist of 4096 x 2048 pixels, resulting in a 12200 x 8600 pixel mosaic. In all frames B (F435W), V (F555W), I (F814W) and Hα (F658N) images are taken. See also Mutchler et al. (2005).

3.1 Available data

In January 2005, the Hubble Heritage Team obtained a set of 4 (B, V, I, Hα) mosaics of the system NGC 5194 (M51) and its companion, NGC 5195, see Fig. 3.1. A color-composite of these images can be seen in Fig. 3.2, and a smaller detail, in which the full resolution can be appreciated, is shown in Fig. 3.3. A full description of the dataset and reduction is given in Mutchler et al. (2005), therefore only a brief description will be given here.

In the different filters, different exposure times are used. Also a smal dithering has been applied to correct for the geometrical distortion and to fill up the chip gaps, using the technique of drizzling (see also Section 3.2). An overview of the different exposure times and corresponding limiting magnitudes are given in Table 3.1. For the dithering, the standard ACS pipeline values are used: 2.5x1.5 pixels and a larger one of 5x60 pixels to span the chip gap.

Figure 3.2:
A color composite of the 4-filter mosaic of M51 and companion. R, G and B colours are made by the I, V and B band respectively. Hα is added to the red image to clearly show the emission of hydrogen, mainly from star forming regions and supernova (super-)bubbles. This image is by far in full resolution. The separate images are scaled, to correct for differences in exposure time, in such a way that they are all about equally visible. Image from http://hubblesite.org/newscenter/newsdesk/archive/releases/2005/12/

3.2 Data reduction

The FITS-files were retrieved from the Multimission Archive at STScI (MAST) after standard pipeline processing, including bias, darkframe and flatfield corrections as well as processing by the `MultiDrizzle` procedure. For details on the standard calibration, see Pavlovsky et al. (2005).

The drizzling procedure is a task that combines multiple dithered images into one clean image. This resulting image is clean of geometrical distortion, cosmic rays and dirty pixels and is corrected for biases, flatfields and darkframes. The point spread function (PSF) is constant over the whole chip. For details on the

Table 3.1: Exposure times and corresponding limiting magnitudes for the four filters used.

Filter	Exposure time	Limiting magnitude
F435W (B)	4 x 680s = 2720s	27.3 m_B
F555W (V)	4 x 340s = 1360s	26.5 m_V
F814W (I)	4 x 340s = 1360s	25.8 m_I
F658N (Hα, [N II])	4 x 680s = 2720s	-

Figure 3.3:
A zoom in to Fig. 3.2. The lower right image is at full resolution. 1 pixel corresponds to 0.05 arc seconds, which is about 2 parsec at the distance of M51, about 8.4 Mpc. A lot of details are clearly visible, like clusters, grouping together in complexes, surrounded by a superbubble, the result of the supernova explosions of the most massive stars.

drizzling procedure, see Fruchter & Hook (2002); Mutchler et al. (2002).

I only use drizzled images in this thesis and therefore I will use this single PSF for the whole mosaic whenever needed. The PSF has been obtained empirically by Marcelo Mora (ESO, Garching) from images of the globular cluster 47 Tuc, separately for every available filter.

3.3 The M51 system

M51 is a Milky Way type Sbc galaxy, and its companion is a dwarf barred spiral of early type SB0. The distance to the system is determined to be 8.4 ± 0.6 Mpc by Feldmeier et al. (1997) from planetary nebulae.

The system is seen almost face on (Tully (1974)). This greatly simplifies determinations of galactocentric distance, as well as whether or not the cluster is in a spiral arm. The height above the galactic plane cannot be determined.

An ACS pixel corresponds to 0".05. At a distance of 8.4 Mpc this corresponds to a distance of 2 pc. This is smaller than typical galactic cluster sizes, which are about 3-4 pc (Spitzer (1987); Kharchenko et al. (2005)). This creates the possibility of 'resolving' the star clusters, with which we mean that we can clearly distinguish stars from clusters by comparing the size of the source with the PSF.

Chapter 4

Deriving cluster parameters

To investigate the properties of the star cluster population of M51 it is important to have a complete unbiased sample in order to get statistically reliable results. In this chapter the whole process of the determination of the different parameters are described. In Sect. 4.1 I describe the selection of point sources. The radii are measured, as described in Sect. 4.2 and the procedure of the photometry fills Sect. 4.3. Sect. 4.6 concerns the selection of the final sample, of which the completeness is discussed in Sect. 4.4. The results are the topic of the next chapter.

4.1 Source selection

Selection of pointlike sources was done with the SExtractor package (Bertin & Arnouts, 1996), version 2.3.2. The image has been smoothed over an area of 10 pixels. For this smoothed area a mean and standard deviation of the intensity are determined. Deviating pixels were iteratively discarded until every pixel was within $\pm 3\sigma$ of the mean value. A source now is defined as a region on the original image where at least 3 adjacent pixels exceeds the background by at least 5σ. The resulting source list in the three different filters were cross-correlated, and only sources within a 2 pixel uncertainty were kept, removing a lot of the remaining noise. The resultant coordinate list contains 75 436 sources.

4.2 Radius determinations

The excellent resolution of the *ACS* camera (1 pixel $\hat{=}$ 0".05) gives us the opportunity to distinghuish clusters from stars, by means of their spatial extent. We use the *ISHAPE* routine within the *BAOlab* package (Larsen, 1999, 2004) to determine the effective radii (projected half light radii) of all point sources. Analytic cluster profiles are convolved with an emperical PSF of the camera. We used two different analytic cluster profiles: a Moffat profile and a King profile, as will be explained below (Sect. 4.2.2).The convolution is compared to the data and χ^2 is determined. By minimizing χ^2 the best fit effective radius can be obtained.

4.2.1 The Point Spread Function

The PSF was obtained from a drizzled image of the globular cluster 47 Tuc. All sources on this image are in fact images of the PSF, so by using isolated stars, which are not saturated, it is not too hard to extract the PSF. Because of the drizzling procedure the PSF is constant over the whole field of view (Mutchler et al., 2002). It differs (mainly in size) per filter, and we therefore use different PSFs for the different filters.

4.2.2 Analytic cluster profiles

We used two different profiles, because different types of clusters are found in galaxies (different populations are better described by different profiles). The first one is a Moffat profile (Moffat, 1969) with a power law index of -1.5. This is very similar to the average profile of young star clusters in the LMC (Elson et al., 1987). The second choice is a King profile (King, 1962) with a concentration parameter (tidal radius over core radius) of 30. This is found to be a good description of old galactic globular clusters (Harris, 1996) and therefore expected to also describe the older M51 clusters rather accurately.

Whereas we try fitting two different profiles, Larsen (1999) has shown that the derived effective radius (via a conversion factor (Larsen, 1999) from the two fit FWHM) differs only marginally.

4.2.3 Cluster fits and precision

We allow the cluster profiles to be elliptic. The orientation as well as the ratio of major to minor axis are free parameters. If a cluster is fit to be elliptic, the resulting effective radius in fact is the semimajor axis of the ellips.

Besides the cluster profile, also a pure PSF fit is applied to the sources. A comparison of χ^2 of this fit and the one of the best fit cluster model can be used as a selection criterium for clusters.

According to Larsen (2004) the minimal cluster size *ISHAPE* can resolve is one with a FWHM of 0.2 pixels. With *ACS*, at the distance of M51, this corresponds to 0.5 pc. We therefore take this as a lower limit. The accuracy of the routine is of the same order.

4.3 Photometry

On all sources on the list created by the SExtractor routine, photometry is performed using the *IRAF/DAOphot* package. An aperture of 5 pixels in radius was used and the background annulus with an inner radius of 10 pixels and a width of 3 pixels.

4.3.1 Aperture corrections

Since we are not dealing here with pure point sources an aperture correction has been applied. Artificial sources have been created using the *BAOlab* package (Larsen, 1999, 2004), with a Moffat profile with power law index of -1.5 and an effective radius of 3 pc. This profile is concolved with the filter dependent PSF. Convolved profiles were used to measure aperture corrections from 5 to

10 pixels ($\hat{=}$ .5 arcsec). The resulting aperture corrections for *F425W*, *F555W* and *F814W* were -0.16, -0.16 and -0.17 respectively. These values would be 0.04 lower/higher for sources which are 1 pc bigger/smaller. Aperture corrections between 0".5 and infinity were taken from Sirianni et al. (2005).

4.3.2 Extinction corrections

All clusters are affected by the same Galactic foreground extinction. We take a value of $E(B-V) = 0.038$ from Schlegel et al. (1998). For accurate local (i.e. in the M51 system) extinction determinations one needs a wide range of broadband photometry, in order to overcome the age/metallicity/extinction degeneracy. Because we only have *B,V,I* photometry we are not able to clearly distinguish the effects. Therefore we do *not* correct for local extinction. A strongly peaked (at $E(B-V) = 0$) power law distribution for extinction values is found by Bastian et al. (2005b) for the cluster population in the central regions of M51. Mean values for A_V are in all age bins around 0.3 (a little smaller for clusters older than 20 Myr, then for the younger ones), with a larger scatter for younger clusters.

4.4 Completeness

In order to have complete, unbiased samples of clusters we perform completeness test with artificial clusters. Because it is to be expected that the completeness fraction is a function of cluster luminosity, cluster size and background intensity (and variation) I will determine 90% completeness limits for three seperated background regions, for different cluster sizes.

The completeness limits are determined on square section of the image of 1000 x 1000 pixels. Artificial sources were added to the image and the same routine applied to fit all sources back. This resulted in 90% completeness limits of 23.3 mag for *F435W* and *F555W* and 23.0 mag for *F814W*.

4.5 Background regions

Because the background intensity is strongly varying over the whole image, especially when comparing spiral arms with the interarm regions, we divided the image in three background levels, as indicated in Fig. 4.1. The image has been smoothed with a Gaussian kernel with a size of 200 pixels. Two isophotes on this smoothed image are used as background limits.

4.6 Sample selection

Finally it's possible to select a sample of clusters for the investigation. Because it has proven much more difficult to obtain a reliable cluster radius than to be sure that a source is a cluster, we will use two seperate samples of sources for the investigation of the radii and for the investigation of luminosities.

For both sets the following conditions should hold:

1. The source is detected in *F435W*, *F555W* and *F814W*;

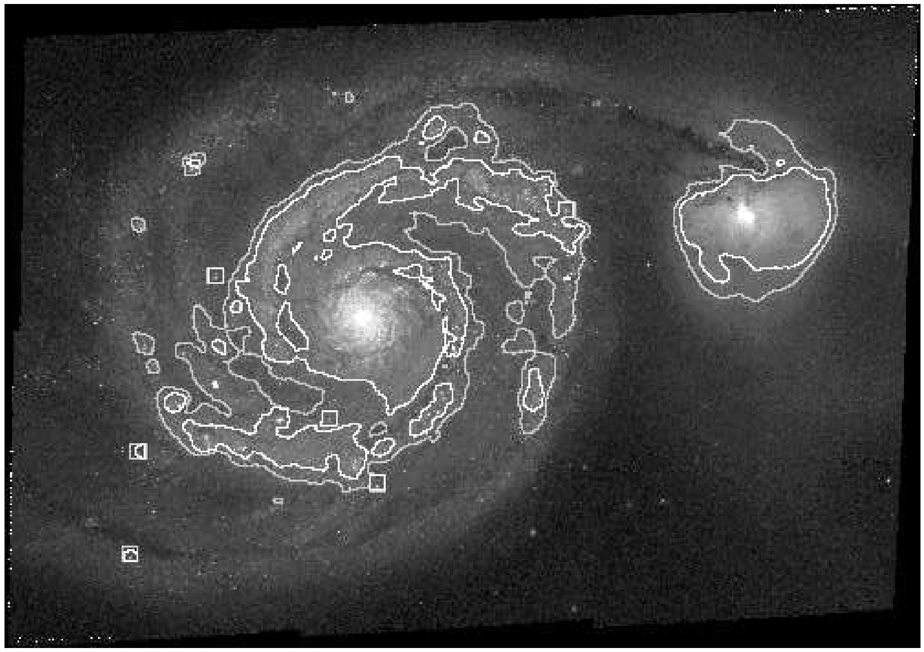

Figure 4.1:
The contours that outline the three background intensity level regions, superimposed on the image in the *F555W* passband. The bright white line encloses the highest background level and everything outside the grey line is called low background. The area in between the white and grey lines is a transition region, to have the other two regions clearly distinguishable.

2. The source is extended, defined as $R_{\text{eff}} > 0.5$ pc, the accuracy of *ISHAPE*;
3. The fit of the cluster profile is better then the fit of a pure PSF, distinguished by means of χ^2
4. The source is brighter than the 90% completeness limit
5. The nearest neighbouring source is at least 5 pixels away, to avoid contamination

These criteria will deliver a complete set of sources of which we can be sure are clusters. In order to also have reliable radius determinations, we have to impose the following extra constraints:

6. The source is on the lowest background region (for reason, see below)
7. The nearest neighbour is at least 10 pixels away

Tests performed by Remco Scheepmaker (private communication) have shown that for clusters in a highly *varying* background the radius determination is rather unreliable. The main problem is that the *ISHAPE* routine considers the background smooth (a mean value with standard deviation which is constant in the ring in which the cluster profile is fit). In the high and intermediate background regions the background is not only high, but also strongly varying. Result is that the best fit model will be a model in which a high background value is fit as being part of the cluster. Other solutions than just ignoring high (and thus highly varying) background regions are currently under investigation. The nearest-neighbour criterium is stronger here, because otherwise light of a neighbouring cluster is inside the region where the cluster profile is determined. This will be have the same effect as a variable background.

The resulting sample used for investigations of radii will therefore be considerably smaller than the sample used for the study of the luminosity function.

Chapter 5

The distribution of M51 cluster radii

This chapter deals with the most interesting distributions and relations with respect to the radii. Implications of the results and discussion are the subject of Chapter 7, here only an overview of observational results is given.

Wherever distribution functions are fit to the data, I also refer to Appendix A, where I describe the fitting procedure of a distribution function in different circumstances and problems with different methods to do so. Main conclusions of that Appendix are that distribution functions are most reliably fit using a Maximum Likelihood method, unless there are several parameters to be fit. In the latter case the Likelihood Function can have several local extrema and the computational time goes as a power law, with the number of free parameters as exponent. Therefore, multiple parameter distribution functions will be fit in a different way, as described in Appendix A.

5.1 Radius distribution function

The study of the radii is at the time of writing of this thesis still under debate. Unreliable radius determinations are the main reason to only put preliminary results in this thesis. Conclusions, in the next chapter, will also be only qualitative.

Because of the very restricting selection criteria, listed in Section 4.6, the resulting complete set of reliable clusters only contains 769 clusters. The distribution of these radii can be seen in Fig. 5.1. As can be seen, there is no fit drawn. It is as yet not clear what a reasonable functional form of this fit should be. Right of the peak, a power law can be fit using a Maximum Likelihood method (see Appendix A). This, although sensitive to fitting limits, gives a power law slope somewhat steeper than 2, as was for M51 also found by Bastian et al. (2005b).

From the fact that the distribution is peaked it is obvious that there is something like a preferred radius. The value is around 3 or 3.2 parsec, which are the median and mean radius, respectively. This is in good agreement with the results of Jordán et al. (2005) for old cluster populations in the Virgo galaxy

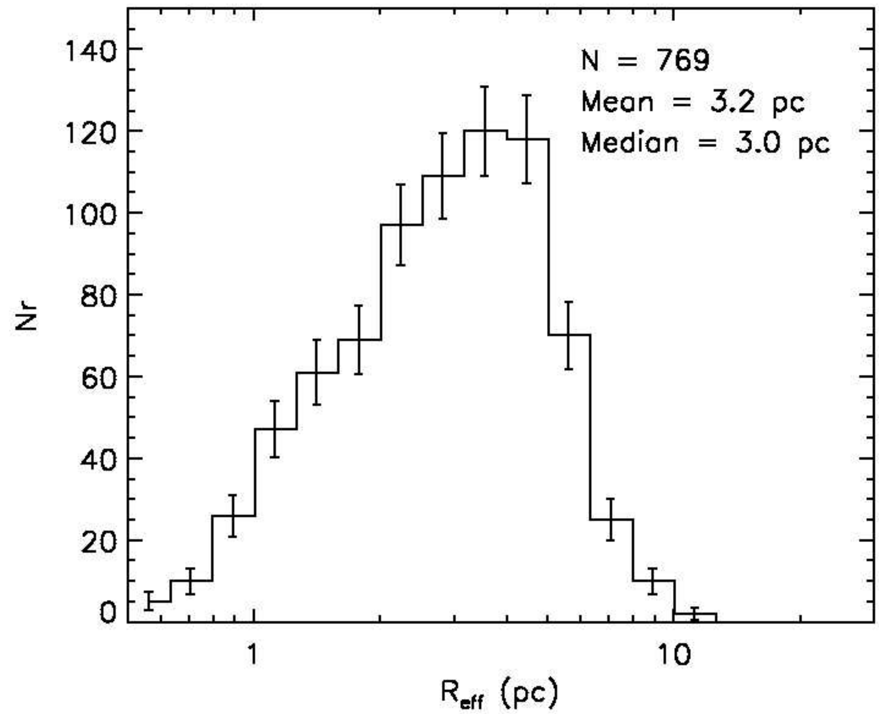

Figure 5.1:
The distribution of radii in M51, with the radius on a logarithmic scale and the number linear. The error bars indicated are poissonian errors resulting from counting statistics. Due to the very restricting selection criteria, as described in Section 4.6, there are only 769 clusters in the sample. For this clusters the radii are trustworhty and it is a complete sample. The location of the peak and the shape of the distribution are therefore statistically justified. Because of the skewness of the distribution the mean and median radius are somewhat different, and are both indicated for future comparison. Figure courtesy of Remco Scheepmaker.

cluster, Harris (1996) for old clusters in our Milky Way and for samples of young clusters, as found by e.g. Larsen (2004).

5.2 Radii throughout the disk

The set of reliable radii is too small to have statistically valuable radius distributions at, for example, different galactocentric radii. We therefore stick to mean radii at different galactocentric distances. The result is show in Fig. 5.2. The red rectangles are mean radii from a sample of clusters with that particular mean galactocentric distance. Although the mean radius increases a little bit, there seems to be just a very weak relation between both parameters. Fitting a powerlaw of the form $r \propto d^x$ gives an exponent of $x \approx 0.1$, indicated by the dashed line in the Fig. 5.2. The mean or, if you like, preferred radius is roughly constant over the whole disk. Note that in the case of M51, we are dealing with an, in general, *young* cluster population, of which the majority of the clusters is formed because of the tidal interaction between M51 and NGC 5195. The solid

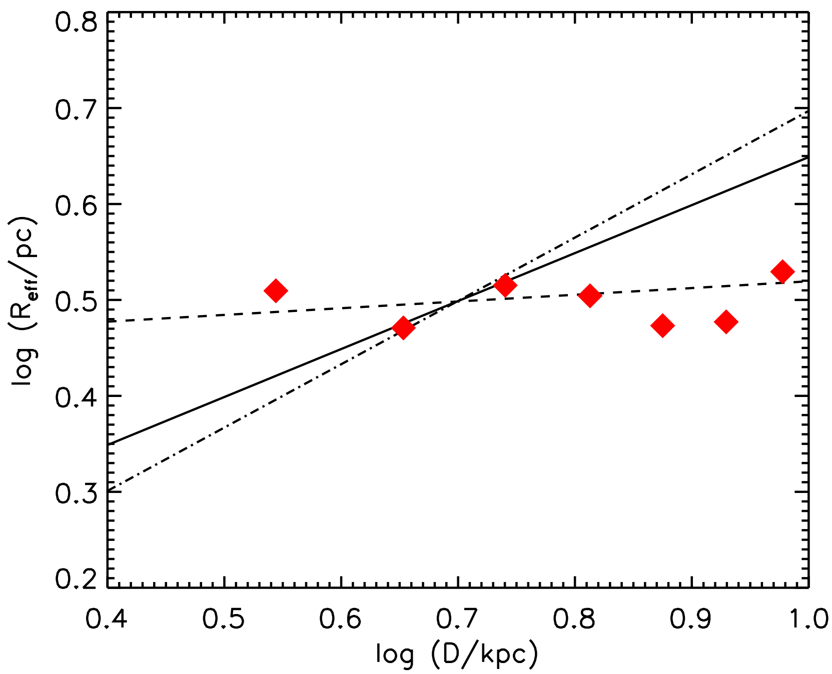

Figure 5.2:
The variation of the mean effective radius with galactocentric distance. The red rectangles are from our observations of M51; the dashed line is a power law fit through them, with a slope of ∼0.1. The solid line is the fit of the Milky Way globular clusters (note: all old clusters), as obtained by van den Bergh et al. (1991). The dot-dashed line is the relation between radius and galactocentric distance for tidal equilibrium of the clusters (of arbitrary mass, varying this mass scales the line vertically, and the scaling is arbitrary anyway), see Equation 2.1. Figure courtesy of Remco Scheepmaker.

line is the (appropriately scaled) best fit for the Milky Way globular cluster system, i.e. an *old* cluster population. The dot-dashed line is the (again appropriately scaled) relation for clusters in tidal equilibrium with their host galaxy, as described in Sect. 2.1, Eq. 2.1. Any changes in the shape of the distribution function cannot be shown significantly.

Chapter 6

Luminosity function

As described in Chapter 2, Section 2.2.2, the luminosity function (LF) is a useful tool in the study of a cluster population, especially if no reliable information regarding masses, ages and extinction of individual clusters is at hand.

The luminosity function in the three different passbands is shown in Figs 6.1, 6.2 and 6.3, in the uppermost panels. The fit results in the three different passbands are summarized in Table 6.1, for a single power law fit as well as for a double power law. The final column in this table gives a comparison of the goodness of both fits using reduced χ^2 of the fits. It is clear that in all cases the double power law function fits better. A comparison of Likelihoods for both fits (see Appendix A) would give a stronger argument, but as I didn't use that method to fit, I keep it with this criterium.

The single power law fits are all in good agreement with previously obtained results for the same galaxy (Bastian et al., 2005b) and other cluster populations (Larsen, 2002; de Grijs et al., 2003a). Double power laws fit better. To make this statement quantitative, see the last column of Table 6.1. As explained in Section 2.2.2, this double power law behavior hints to a truncation of the cluster initial mass function (CIMF) at the high mass end. Discussion on this topic is reserved for the next Chapter (7). A double power law, with similar slopes was already found for M51 by Gieles et al. (2006c). Here we use a slightly different sample and another fit method, and we still obtain similar results. This strengthens the claim that the LF indeed *is* a double power law, instead of a single one. Whitmore et al. (1999) found for the 'Antennae' a double power law, of which the slopes on both sides of the bend are similar to our results, although the bend is at a higher luminosity.

A side remark on the location of the bend: Gieles et al. (2006c) corrected for mean local (i.e. in the M51 system) extinction. Since no reliable estimates for local extinction can be made I do not correct for local extinction here, only for foreground extinction, as described in Chapter 4.

6.1 Relations between LF parameters and location

Because of the size of the cluster sample we have, especially if we are only interested in luminosities and do not care about *reliable* radius determinations, we can divide the sample in certain subsamples. This section describes a few such attempts and the results. Discussion on the results will be given in Chapter 7.

6.1.1 Luminosity functions in different environments

When examining only luminosities of clusters, we just have to be sure that the source is extended and only the first five selection criteria mentioned in Sect. 4.6 should hold. Therefore it *is* possible to make LFs of subsets of the cluster population. An interesting feature appears when we divide the sample in three more or less equally sized subsamples in concentric rings, like shown in Fig. 6.1, 6.2 and 6.3, for *F435W, F555W* and *F814W* respectively.

Two interesting trends are visible in all three passbands. In the first place, the location of the bend shifts to fainter magnitudes if one moves out in the disk. Secondly, the slope of the faint end side of the LF gets shallower when moving inwardly. The results are summarized in Table 6.2. Although the results clearly show a trend, the statistics might raise some doubt. Because the different distance bins show bend locations that are not any more than about 1-4 σ apart, the reader might not be convinced by every single passband on itself. The fact, nevertheless, that we see the same trend in all three passbands indicates that we are looking at a physical, instead of statistical, effect.

In Fig. 6.4 the LF is shown for two different background regions (as described in Sect. 4.4). Results are similar for the other two filters. The intermediate background region is left out, because of the low number of clusters. Almost no variation with background region is found for the location of the bend. In the example given (Fig. 6.4), the location differs by $\sim 1\sigma$. This is typical also for the other two passbands. The slope at the faint end of the LF, nevertheless, is significantly shallower for the clusters on the high background than for clusters on a low background. These slopes are significantly different; they are seperated by tens of standard deviations, and so require a physical explanation.

In summary, the results of an investigation of relations between LF parameters and location are:

1. The bend in the LF occurs at *brighter* magnitudes, *closer* to the center of the galaxy

Table 6.1: Fit results of the whole sample in all three pass bands. Every cluster with $m < 23$ is taken into account in the fits. The first column is the passband, the second the number of clusters within the fit range. Column three contains the slope of the single power law fit, whereas the fourth, fifth, sixth and seventh column contain the both slopes and the location of the bend of the double power law respectively. De final column shows the ratio χ^2_d/χ^2_s of the goodness of both fits in terms of chi squared, comparing the single and double power law distribution functions.

		Single PL	Double PL			
Filter	N	α	α_1	α_2	$M_{\rm bend}$	$\frac{\chi^2_d}{\chi^2_s}$
*F*435*W*	3891	2.18 ± 0.02	1.96 ± 0.04	2.52 ± 0.08	-8.33 ± 0.15	0.63
*F*555*W*	4750	2.19 ± 0.02	1.99 ± 0.04	2.56 ± 0.07	-8.38 ± 0.13	0.67
*F*814*W*	8041	2.18 ± 0.01	2.08 ± 0.02	2.54 ± 0.08	-8.90 ± 0.16	0.77

2. The location of the bend in the LF is largely *independent* of background intensity

3. The slope of the faint end side of the LF is *shallower, closer* to the center of the galaxy

4. The slope of the faint end side of the LF is *shallower* in *high* background regions

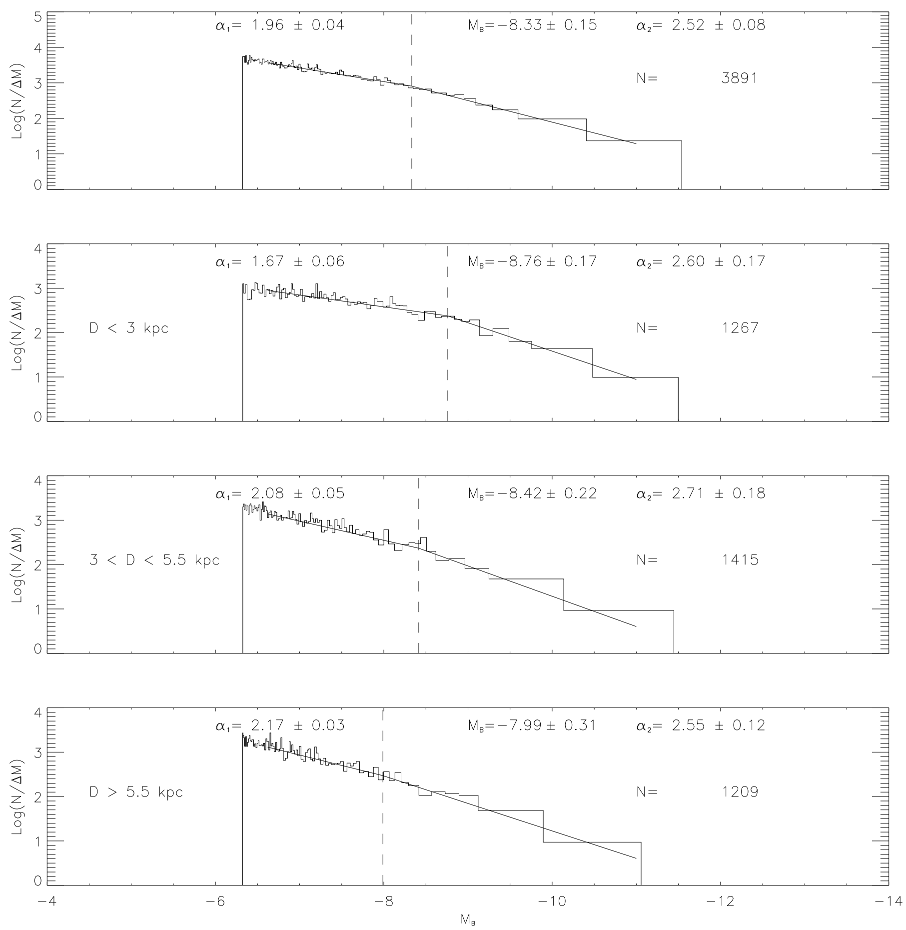

Figure 6.1:

The luminosity function of clusters in M51 in M_{F435W} which fulfill the criteria listed in Section 4.6 with a magnitude brighter dan m_{F435W} = 23.3. The double power law fits are performed on all clusters brighter than m_{F435W} = 23. Only clusters with a galactocentric distance less than 8.4 kpc are in this sample (in order to exclude clusters belonging to NGC 5195). The top panel is the whole sample, the lower three plots are three, in number more or less equally divided, samples, at different galactocentric radii. Both slopes as well as the position of the bend are indicated (vertical dashed line).

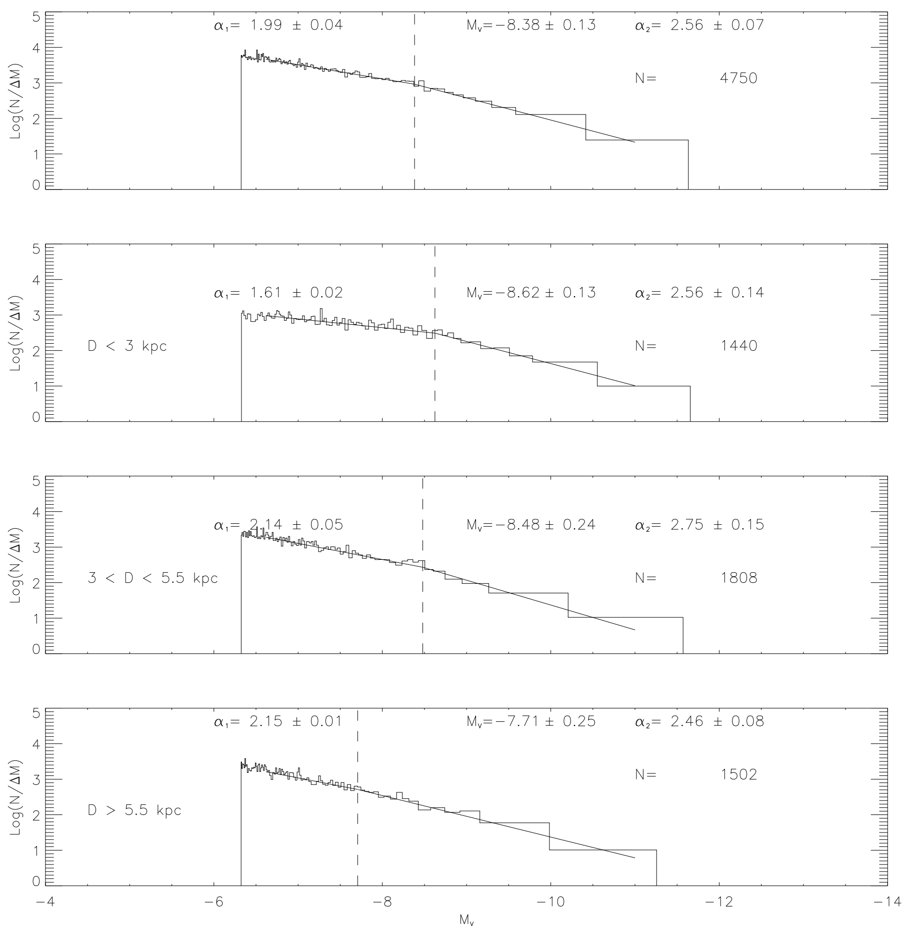

Figure 6.2:

The luminosity function of clusters in M51 in M_{F555W} which fulfill the criteria listed in Section 4.6 with a magnitude brighter dan $m_{F555W} = 23.3$. The double power law fits are performed on all clusters brighter than $m_{F555W} = 23$. Only clusters with a galactocentric distance less than 8.4 kpc are in this sample (in order to exclude clusters belonging to NGC 5195). The top panel is the whole sample, the lower three plots are three, in number more or less equally divided, samples, at different galactocentric radii. Both slopes as well as the position of the bend are indicated (vertical dashed line).

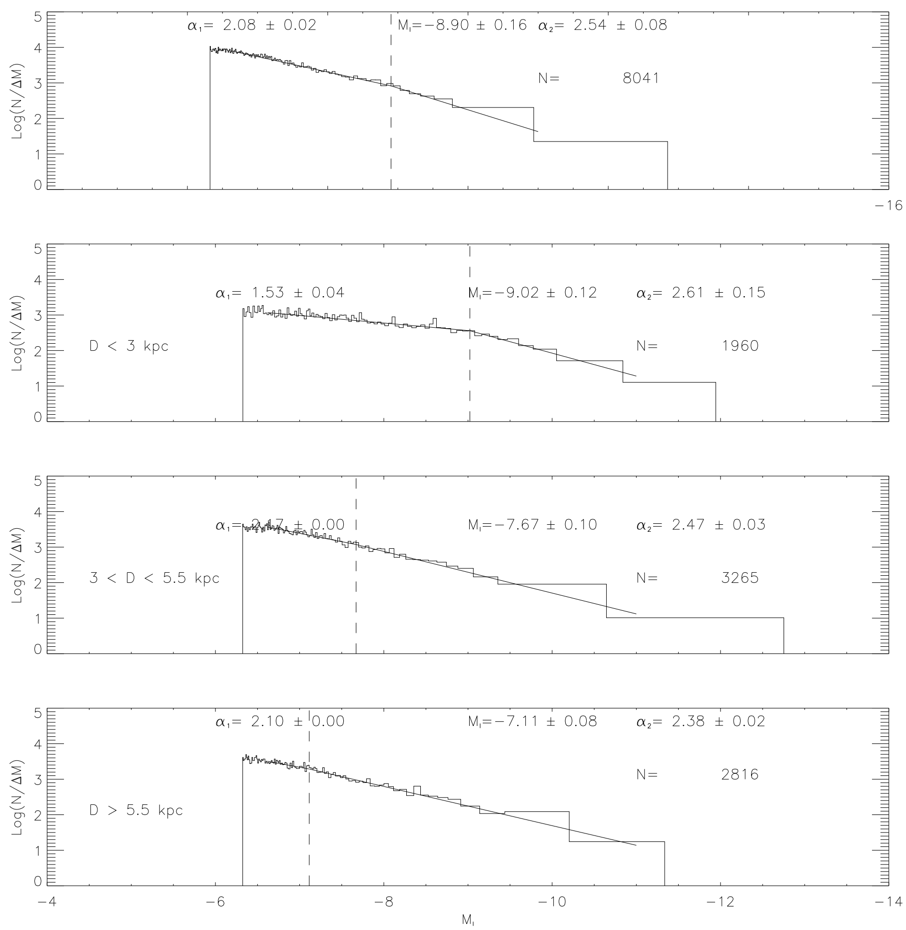

Figure 6.3:

The luminosity function of clusters in M51 in M_{F814W} which fulfill the criteria listed in Section 4.6 with a magnitude brighter dan $m_{F814W} = 23.3$. The double power law fits are performed on all clusters brighter than $m_{F814W} = 23$. Only clusters with a galactocentric distance less than 8.4 kpc are in this sample (in order to exclude clusters belonging to NGC 5195). The top panel is the whole sample, the lower three plots are three, in number more or less equally divided, samples, at different galactocentric radii. Both slopes as well as the position of the bend are indicated (vertical dashed line).

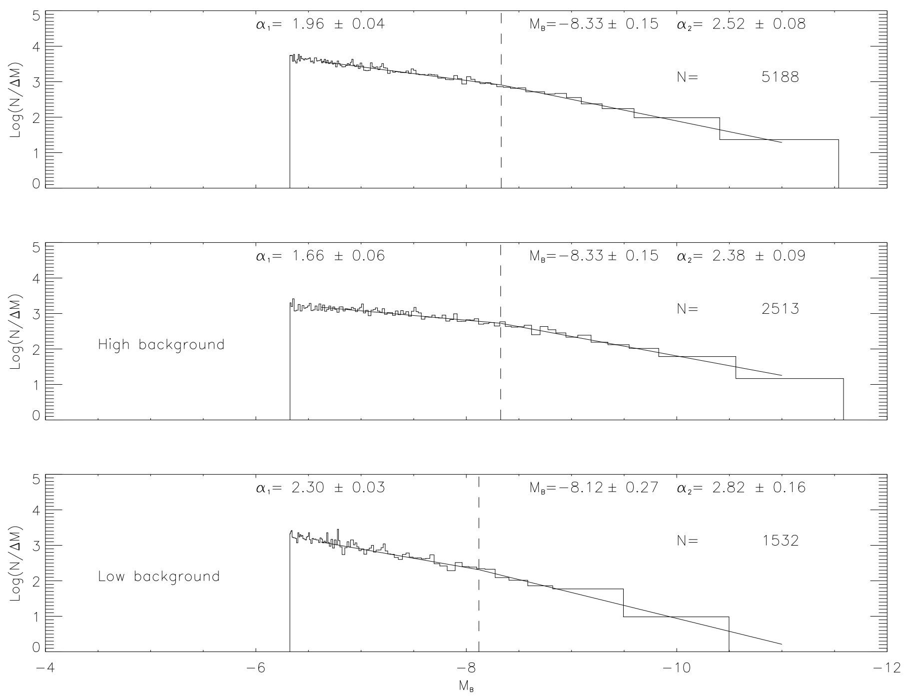

Figure 6.4:
The luminosity function of clusters in M51 in M_{F435W} which fulfill the criteria listed in Section 4.6 with a magnitude brighter dan m_{F435W} = 23.3. The double power law fits are performed on all clusters brighter than m_{F435W} = 23. Only clusters with a galactocentric distance less than 8.4 kpc are in this sample (in order to exclude clusters belonging to NGC 5195). The top panel is the whole sample, the lower two plots are the clusters from the high and low background intensity regions, as indicated. Both slopes as well as the position of the bend are indicated (vertical dashed line).

Table 6.2: Results of fitting a double power law distribution to several subsets, more or less equally divided in number. Three subsets at different galactocentric radii are fit. For all three passbands both the slopes as well as the location of the bend (in the magnitude of the filter in question) are given. Trends are similar in the three different filters, strengthening the credibility of the effects.

Filter	D (kpc)	α_1	α_2	$M_{\rm bend}$
$F435W$	0 - 3	1.67 ± 0.06	2.60 ± 0.17	-8.76 ± 0.17
	3 - 5.5	2.08 ± 0.05	2.71 ± 0.18	-8.42 ± 0.22
	5.5 - 8.4	2.17 ± 0.03	2.55 ± 0.12	-7.99 ± 0.31
$F555W$	0 - 3	1.61 ± 0.02	2.56 ± 0.14	-8.62 ± 0.13
	3 - 5.5	2.14 ± 0.05	2.75 ± 0.15	-8.48 ± 0.24
	5.5 - 8.4	2.15 ± 0.01	2.46 ± 0.08	-7.71 ± 0.25
$F814W$	0 - 3	1.53 ± 0.04	2.61 ± 0.15	-9.02 ± 0.12
	3 - 5.5	2.17 ± 0.00	2.47 ± 0.03	-7.76 ± 0.10
	5.5 - 8.4	2.10 ± 0.00	2.38 ± 0.02	-7.11 ± 0.08

Chapter 7

Implications and speculations

This chapter is devoted to giving some discussion on the results obtained. Because all of the described projects are still part of ongoing work, the distinction between implications and speculation can be a bit vague. Conclusions described in this chapter are descriptions of how I think the results should be interpreted, at the time of writing of this thesis. This is likely to change in due time.

7.1 Cluster sizes

The clusters in M51 seem to have a distribution function peaked around 3 pc. This is comparable to what the globular clusters in our galaxy show (van den Bergh et al., 1991). Jordán et al. (2005) report on the radii of star clusters of galaxies in the Virgo cluster. They show that an appropriate scaling of the radius distribution function, as a function of the intrinsic color of the galaxy, makes the peaks of all their populations come together. The preferred cluster radius seems to be related to the color of their host galaxy. The Virgo cluster consists of elliptical galaxies, all with old cluster populations. As is shown by Scheepmaker et al. (2006), the same color correction on the size distribution of our young cluster population in M51, makes the peak of our distribution coincide with the old populations of Jordán et al. (2005). This is very remarkable as it might indicate that the peak of the radius distribution function is subject to some kind of evolution, closely linked to the evolution of the host galaxy.

An important difference between the old cluster population of our galaxy and the relatively young population in M51 is the size distribution as a function of galactocentric distance. Where the old population shows a relation close to tidal equilibrium, our younger population shows hardly any relation at all. This also can be an evolutionary issue: clusters are born with a more or less random radius, peaked around some preferred radius and slowly evolves towards an equilibrium with the host galaxy. Old populations had much more time to adapt to the tidal field (cluster relaxation times are of the order of 10 Gyr for globular cluster like masses) and therefore they are on their way evolving into this equilibrium. It would be interesting to see also intermediate cases.

The fact that no relation is found between cluster radius and background intensity can also be explained. If one would have obtained a relation between both, it would mean that we could see the effect of cluster stretching and squeezing in e.g. spiral arms (see Chapter 2). This stretching and squeezing mainly affects the outer region of clusters, leaving the nucleus comparatively undisturbed. Because we determined half-light radii, the clusters nucleus emits the main part of the light that is used for size determinations. Gieles et al. (2006a) have shown that the clusters half mass radius is much less affected by dynamical distortions when being in interaction with spiral arms than is the 'outer' radius.

7.2 Maximum cluster mass, star formation and cluster disruption

From the statistical significance of the double power law fit to the LF (compared to a single power law) we infer, on grounds of the models developed in Gieles et al. (2006b) and shortly explained in Sect. 2.2.2, that there exists a physical upper mass limit for star clusters in M51. I do not make any statement about the exact value for this truncation for the following reasons. In the first place this is sensitive to the formation rate of the clusters, which I also did not derive from the observations. Secondly, the conversion of the location of the bend in magnitudes to a truncation of the mass functions implies that this bend is exactly there where it is. Instead, we have no reliable cluster-by-cluster extinction information, and therefore this bend is supposed to be shifted by the mean extinction (which is expected to be about 0.3 magnitudes in the *F555W* passband, based on extinction in the central region of M51, as derived by Bastian et al. (2005b)).

The question now *is*: why is there a maximum mass for star clusters? Is there really a mass gap between the most massive star clusters and dwarf galaxies? Is this expected to be different in different galaxies? We can get hints to the answers to these questions from the obtained dependencies of the location of the bend on galactic position, as derived in Chapter 6, Section 6.1.1.

The question of maximum mass is closely related to the formation of clusters. Of course a maximum possible mass for Giant Molecular Clouds results in a hard limit on a maximum possible cluster mass. In reality, however, one GMC tends to form a whole complex of clusters, see e.g. Bastian et al. (2005a). These complexes are large, but not large enough the sample the whole mass function, until a possible truncation (for which one easily needs several thousands of star clusters, depending on the slope of the mass function and the exact value of the truncation).

7.2.1 Mass limits at various locations

The variation of the location of the bend tells us that this upper mass limit is lower, further out in the disk. There, the bend occurs at a lower luminosity. Molecular clouds at those locations are larger, and therefore also more massive (because of the hydrostatic equilibrium between mass and radius). Shear effects, resulting from the differential rotation of a flat-rotation-curve disk, on the clouds are apparently not that important. Shear effects are larger in the inner regions of the galaxy. The *size* of a cloud is therefore limited to a smaller value in the inner regions. Because clouds are in hydrostatic equilibrium, their size and mass scale with each other. Result is that clouds in the outskirts of the galaxy can in principle be *more massive*. From the fact that cluster can get more massive in the *inner* regions we infer that cloud masses do *not* constrain the mass of the cluster. This can be understood from the fact that a large cloud transforms into a complex of clusters, rather than one single cluster.

Elmegreen (2002) and Elmegreen & Elmegreen (2001) already predicted a maximum mass for star clusters, which should depend on the pressure in clouds. Stars and clusters form from turbulent clouds (Krumholz & McKee, 2005), where the gravitional forces are partly balanced by large scale turbulent motions.

It has been suggested that the mass of a star cluster depends on the cloud core pressure and density as

$$M \propto P^{3/2} n^{-2} \tag{7.1}$$

With a maximum cloud core pressure, this would result in a maximum mass. This mass limit is expected to be higher in the central regions of a galaxy, and in spiral arms (so basically in the high background region), because there the surrounding pressure is higher as well. The dependency on background is only marginally found. This can be explained by the fact that once the cluster formed (all within a high density region!) they move out of the spiral arm and only later come back in. Because thegalactocentric distance of an orbit is more or less constant the dependency on galactocentric distance is much more profound.

7.2.2 Cluster disruption at different sites

The slopes of the faint ends of the different LFs get steeper outward. If the decrease of the slope is interpreted as the result of mass dependent disruption of star clusters (see e.g. Baumgardt & Makino (2003); Boutloukos & Lamers (2003); Lamers et al. (2005)), then it is clear that the typical disruption time is shorter in the inner parts of a galaxy. Regions of higher surrounding densities, where encounters are more frequent, are regions where clusters are destroyed. Therefore the destruction rate of cluster in high density regions appears as a much flatter faint-end-slope in the LF.

Chapter 8

Outlook

Of course the work is not finished here. In the first place, better radius determinations (and therefore a more reliable sample of cluster sizes) will be available soon and thoroughly investigated (Scheepmaker et al., 2006). Comparison with the work of Jordán et al. (2005) seems very promising.

With respect to the LF, it would be interesting to not only compare different regions in one galaxy, but also intercompare galaxies. One cannot choose every galaxy to look for a bend in the LF. One needs a large galaxy with a comparatively high star formation rate (per unit area) in order to have a large sample of cluster, in which in principle the mass function would be sampled all the way up to the statistical limit. If the physical limit, then, is lower than this statistical one, it will appear as a bend in the LF. Dependencies of the value of the maximum mass upon host galaxy type, ambient density and so on will shed a brighter light on the exact cause of the upper mass limit.

Appendix A

Power law distribution functions

In this appendix several issues regarding power law distributions functions will be adressed. In order to obtain simulations of cluster samples, or stars within a cluster (which have masses distributed more or less like the Salpeter mass function, for example), it is important to be sure that the quantities one puts in his simulations are really distributed in the way you want it. When doing this analytically, you neglect the intrinsic statistical nature of distribution functions. Therefore, a good way of creating a sample of stars or clusters is by random sampling a distribution function.

On the other hand, you can have a dataset with data. When you expect these data to be power law distributed, you want to fit a power law distribution function. As I will show in this appendix, this is not as trivial as it may seem. Binning the data is dangerous and almost always resulting in too shallow slopes. Several methods will be compared, making use of a Monte Carlo simulations using random samplinging of the distribution function.

I will here describe everything for the case of a radius distribution function, but everything will remain the same if the variable is changed to for example mass or luminosity. This is partially true also for the fact that I will assume all these distribution functions to be a power law with a negative exponent. Of course functional dependencies will change when this form is changed (and sometimes it is even not possible to do everything analytically), but the methods can in principle be applied to any other kind of functions. In the rest of this appendix distribution function will be abbreviated by DF and PLDF will mean power law distribution function.

A.1 Distribution functions

Distribution functions describe how different values for the (in our case) radius are distributed over all possible values. In the case of a power law with negative exponent this means that there are lots of small clusters and less large clusters. The form in which this usually is written is

$$N(r)\mathrm{d}r \propto r^{-\eta}\mathrm{d}r \tag{A.1}$$

This simply means that the number of objects wit a radius between r and $r + \mathrm{d}r$ is proportional to $r^{-\eta}$ and η is usually called the power law exponent, but 'slope of the power law' is also much heard. The normalization constant that will change the proportionallity into an equality is determined by the total number of objects.

The real number of objects between r_1 and r_2 is given by integration of Eq. A.1:

$$N(r_1 < r < r_2) = \int_{r_1}^{r_2} N(r)\mathrm{d}r = \frac{C}{1-\eta}\left[r_2^{1-\eta} - r_1^{1-\eta}\right] \tag{A.2}$$

in which C is the normalization constant. The mean of a certain quantity $X(r)$ can be found using the following relation:

$$\overline{X} = \frac{\int_0^\infty N(r)X(r)\mathrm{d}r}{\int_0^\infty N(r)\mathrm{d}r} \tag{A.3}$$

It is clear that such a DF is only an exact description of nature if one has an infinitely large sample of objects. It is only defined differentially. The value of a DF is meaningless, only when it is integrated it becomes a physical quantity.

A.2 Random sampling a distribution function

Suppose you want to simulate a cluster population with radii distributed according to a PLDF with negative exponent. This in principle can be done totally analytically. If one starts counting at the largest cluster with $i = 1$, then for the radius of the i'th cluster you can write

$$\int_{r_i}^{\infty} rN(r)\mathrm{d}r = C\int_{r_i}^{\infty} r^{1-\eta}\mathrm{d}r = \frac{C}{\eta-2}\cdot r_i^{2-\eta} = i, \qquad (i = 1, 2, 3, ...) \tag{A.4}$$

Doing so would result in a perfectly distributed range of radii. The random nature of a distribution function, however, has disappeared. Every sample with the same number of clusters would have exactly the same sizes of clusters in it. This is of course highly unlikely. A possibility to change this, and make Eq. A.4 more random is to let i in the righthand side of the equation be randomly varying between for example $i-0.5$ and $i+0.5$. This would help a great deal (the radii of clusters will most likely be different) but it still has an important shortcoming. In reality in just a small sample of clusters it is unlikely, but possible, to have one huge cluster, that seems to fall far beyond the distribution of the other clusters in the sample. The chance that this happens again is proportional to the DF and therefore, if you have enough small samples, in the end everything will average out and you are left with perfectly PLDF distributed clusters. When using a 'random' version of Eq. A.4 this will not happen (unless you make your random version quite complicated).

An easier way to get a sample according to a DF is using a random sampling technique. This is a technique that can be used no matter what functional form the DF has and can be used with or without pre-determined upper and lower boundaries for the radius (or mass, or luminosity, or...).

A recipe for this technique is as follows (for an example, see Section A.3). The DF needs to be converted to a probability density function, or PDF for short. This means that the normalization is now chosen such that the integral of the function from the lower possible limit to the upper one gives the value 1. For a DF this simply means that the old constant (C) is now divided by the total number of objects in the sample. If one wants to use a lower and upper limit, then the integral between these limits should give 1:

$$\text{PDF}(r)\mathrm{d}r = \frac{C}{N} \cdot r^{-\eta}\mathrm{d}r \quad ; \quad \int_{\text{lower limit}}^{\text{upper limit}} \text{PDF}(r)\mathrm{d}r = 1 \tag{A.5}$$

The power of the random sampling technique is hidden in the *cumulative* PDF (CPDF for short). This is the integral of the PDF from the lower limit to a certain radius. If this radius is chosen to be equal to the lower limit it obviously gives 0, and if it's chosen to be the upper limit, it necesserily becomes 1. All possible values will be in the interval $[0, 1]$:

$$\text{CPDF}(r) = \int_{r_{\min}}^{r} \text{PDF}(r)\mathrm{d}r \in [0, 1] \tag{A.6}$$

If you now draw a random number between 0 and 1 (for example using the IDL `randomu` function), you can interpret this as the value for the CPDF and invert the function to see what value for the radius belongs to it. In this way one can convert an array of random numbers between 0 and 1 into radii which are distributed according to any DF you like. In this way the resulting array is really random and it also represents your DF properly. All the above mentioned problems are solved.

Possible disadvantages of the method can arise in several ways. The first is a non-integrable PDF (an example of this is a Schechter (1976) function as DF as is sometimes used to describe cluster mass functions (e.g. Gieles et al. (2006b); Whitmore et al. (1999))). In that case you will have to do the integrals numerically. If you want your array to be as random as possible, you will have to evaluate the integral in very many points. Otherwise the inversion of the CPDF will be only available for a restricted number of 'random numbers' and the resulting arrays of radii will only contain that many different values for the radius. Not very random again...

A second kind of problem can arise when someone is using this techniques for stellar mass functions. If you want to fill a low mass cluster with stars, according to a Salpeter mass function (with a cluster mass lower than the highest possible stellar mass), there is a non-zero possibility that your star is more massive than the pre-determined cluster mass. This of course is not very physical, but can fortunately be overcome quite easily.

A.3 Fitting a distribution function

In this section I will first with a concrete example show the use of the CPDF as explained in the previous section. Once that is done, i will proceed with fitting the distribution back in several ways. It will then become clear that this fitting can bring along serious problems and can give wrong results. The reason for the chosen fitting method in this thesis will become clear.

A.3.1 Creating an array of masses

In this example the masses of stars will be the quantity that are to be distributed according to a PLDF with exponent $-\alpha = -2.35$, also called a Salpeter (1955) mass function (in the whole thesis I use η for the exponent of a radius DF and α for the exponent of a mass function). We take a cluster of given mass and put stars in it with masses, randomly sampled from this Salpeter mass function. The mass function of the stars is now given by

$$N(m)\mathrm{d}m = C\, m^{-2.35}\mathrm{d}m \tag{A.7}$$

in which the constant C can now only be determined from the total mass (the cluster has a given mass, not a given number of stars), using Eq. A.3:

$$M_{\mathrm{cluster}} = C \int_{m_{\mathrm{min}}}^{m_{\mathrm{max}}} m^{1-\alpha}\mathrm{d}m \tag{A.8}$$

$$C = \frac{(2-\alpha)M_{\mathrm{cluster}}}{m_{\mathrm{max}}^{2-\alpha} - m_{\mathrm{min}}^{2-\alpha}} \tag{A.9}$$

Now it is easy to construct the CPDF with this normalization. The big advantage of using a PLDF is that everything can be done analytically.

$$\mathrm{CPDF}(m) = \frac{1}{m_{\mathrm{max}}^{1-\alpha} - m_{\mathrm{min}}^{1-\alpha}}\left(m^{1-\alpha} - m_{\mathrm{min}}^{1-\alpha}\right) \tag{A.10}$$

So if you take a random number from a random number generator and you interpret this as the value for the CPDF, then a random mass, sampled from a PLDF is given by

$$m = \left[\mathrm{CPDF}\cdot(m_{\mathrm{max}}^{1-\alpha} - m_{\mathrm{min}}^{1-\alpha}) + m_{\mathrm{min}}^{1-\alpha}\right]^{\frac{1}{1-\alpha}} \tag{A.11}$$

If one now applies this formula to a series of random numbers one obtains a series of masses. These masses are distributed according to a power law with slope $-\alpha$. If you do so you get for example, for a 10^4 $M_\odot$cluster, Fig. A.1. The used power law slope is -2.35 to obtain a power law sample of stars. In the figure both a log-lin plot and a log-log plot are shown. Only bins equal in size in a linear scale are used. For the stellar masses the upper and lower limit respectively are 0.25 $M_\odot$ and 200 $M_\odot$.

Now there are several ways of fitting back this power law. Because we are here dealing with simulated data, we know exactly what is in the sample. Therefore, fitting this back using different methods can give us quantitative insight on the reliability of the methods. We will test four different methods of fitting, two of which fit binned arrays of data, and two without any binning involved.

A.3.2 Fitting a power law on binned data

Linear bins

Binning the data in bins that are equally sized (linear) is the most straightfoward method and is often used in the literature. The reason for this is that is very easy to fit a power law to these data, by just a linear fit:

$$\log N = \log C - \alpha \log M \tag{A.12}$$

No matter what fit procedure is used, one directly obtains a value for both the normalization constant (C) and the power law exponent (α), including errors.

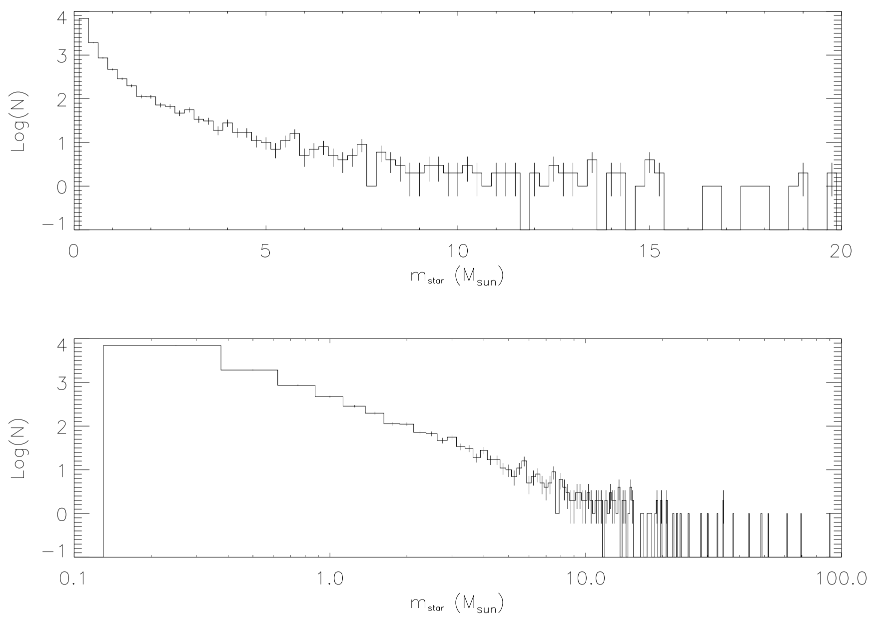

Figure A.1:
The sample of stellar masses created with the method of random sampling, as described in Section A.2. In the upper panel the logarithm of the number in the bin is plotted against the stellar mass on a linear scale. In the lower panel the stellar mass scale is made logarithmic (to see the power law behavior a bit better). The errorbars are the poisonian errors on the number of datapoints in a bin. The used power law exponent is -2.35 and the lower and upper stellar mass limits are 0.25 $M_\odot$ and 200 $M_\odot$ respectively.

Already here you should be careful. Because on both sides of the equation there are logarithms, it is very tempting to bin the masses in logarithmic bins (i.e. in bins which are of the same size on a logarithmic scale). As already noted by Bastian et al. (2005b) this will end up in a wrong value of the powerlaw exponent, namely exponent = 1− slope. This extra 1 arises from the conservation of numbers: $N(\log m)\mathrm{d}(\log m) = N(m)\mathrm{d}m = Cm^{-\alpha}\mathrm{d}m = Cm^{1-\alpha}\mathrm{d}(\log m)$.

The first fit will thus be a fit of a straight line to the logarithm of linearly binned data. The linear bins are already visible in Fig. A.1. With the IDL procedure `linfit` a linear fit is performed on these bins. The errors on the datapoints are given by the poissonian errors on the number of clusters in a bin. The fit results are visible in Fig. A.2.

The first thing that strikes the eye is of course the fit result. The number is much lower than the expected Salpeter value. How can this be? What is the reason for the bad fit? As you can see from the fitted line, it is best for the low mass bins, and much worse for the higher masses. This is because the relative errors on the low mass bins are smaller than the relative errors on the high mass bins (the error is just the poissonian error, and therefore equal to the square root of the number of stars in the bin). Therefore the statistical weight of the lower mass bins is much higher and fit is sort of ‘forced’ to go through these

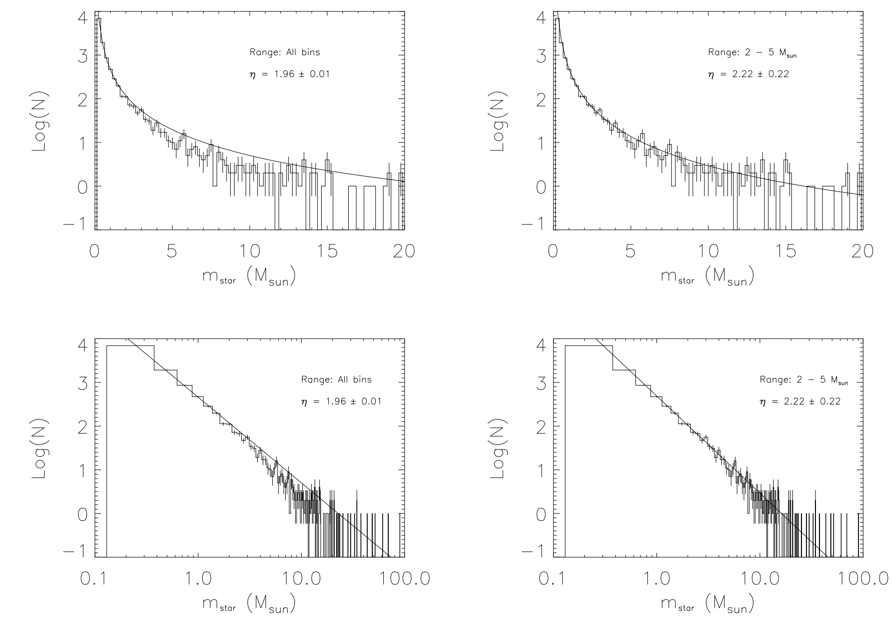

Figure A.2:
The results of a fit on the data using linear, equally sized bins. In the left column you can see the results for the fit if the fit is performed on all the available clusters. It is obvious that, especially on the high mass end, the deviations are large. In the column on the right side the fit is performed on only the bins from 2 to 5 $M_{\odot}$. The fit already is better. The slope is closer to the expected Salpeter value, whereas the fit errors are larger (mainly because of the low number of bins used). Of course it is not desirable to have a fit which depends on the range of fitting.

bins. That is already overcome partly by fitting on a part of the bins, instead of all of them, and then especially ignoring the lowest masses. This is also done in Fig. A.2, in the righthand panel. Only stars with masses between 2 and 5 $M_{\odot}$ are taken into the fit. The result is already much closer to the Salpeter value. We are, however, ignoring the majority of the stars (which are after all of the lowest masses), and therefore the error on the result is also bigger already. Besides that, you don't want to use just a small fraction of your data to obtain a better fit. The worst thing, to end with, is that you really don't want to adapt your fit range to a desired result. We will look into other ways of fitting a PLDF.

Variable binsizes

The main problem with equally spaced bins were the statistical weights assigned to the bins, forcing the fit through the lower mass bins. A way to avoid this is making all the bins equally high (containing the same number of stars), resulting in poissonian errors which are the same for all bins. Of course the bins are not equally spread anymore. The width of the bins increases to higher masses and the information of the power law is now stored in the spacing of the bins instead of in the height of the bins. This method is explained in more detail by Maíz

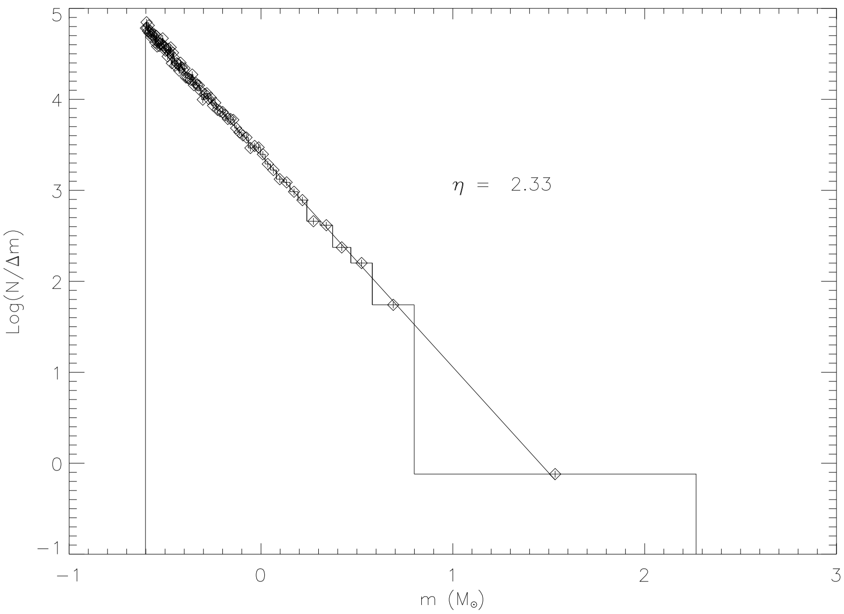

Figure A.3:
The result of the fit of the fit using the method with bins of equal height. No bins are drawn, but rather diamonds at the center of the bins, with the (poissonian) errorbars inside them. The quantity on the vertical axis is the logarithm of the number of stars in a bin (which is the same for each bin) divided by the width of the bin (which is an increasing number towards higher masses). Even for the high mass bins the fit goes reasonably well through the points, resulting in a very good χ^2 (1.05).

Apellániz & Úbeda (2005). To these bins a power law function is fitted using the `curvefit` procedure in IDL.

For this fit a couple of 'rules' are taken from Maíz Apellániz & Úbeda (2005), who have taken it from D'Agostino & Stephens (1986). The first one is the number of bins, which for a sample of $N_{\rm obj}$ objects is preffered to be

$$N_{\rm bins} \approx 2 \cdot N_{\rm obj}^{2/5} \tag{A.13}$$

The result of the fit can be seen in Fig. A.3. On the vertical axis, now, there is not the number of stars per bin, for that would result in a horizontal line, but rather the number of stars in the bin divided by the width of the bin. In that way you mimic the PLDF to make it comparable to previous figures.

A first conclusion is that the fit is already far better than before. The slope is almost right and visual inspection of the figure learns that the line goes reasonably well through all the bins. Because of the relatively large number of bins and the fact that the error on a bin results only from the number of stars in it (and not on the binwidth) the relative errors are small.

A.3.3 Fitting methods without binning

This is easy to understand by the fact tha t binning smooths the data. In a PLDF with negative slope, datapoints are concentrated on the left side of the bin. Therefore smoothing/binning always makes the data appear to be a little bit more to the right. Doing so in every bin makes the total distribution appear flatter than it really is. To get rid of this problem altogether one can also try a method of fitting a PLDF to these data without involving any binning at all. Here I will describe two such methods.

The cumulative mass spectrum

One possibility is using a function that looks very much like the CPDF and is described in detail by Rosolowsky (2005). In short the method is as follows. A DF is defined such that for every mass (m') you can calculate how many stars there should be with a mass higher than or equal to that mass:

$$N(m \geq m') = C \int_{m'}^{\infty} N(m)\mathrm{d}m \tag{A.14}$$

with C determined from the total number of stars. This function then has the value 1 for the most massive star, 2 for the one but most massive, 3 for the third in line, and so on. In the case of a PLDF this function is analytically easily solved. Big advantage of this method is that it involves no binning at all, so you don't have to care about things like statistical weights, poissonian errors and so on. A second advantage is that it is very easy to also fit a possible truncation to the mass function, by replacing the infinity symbol in Eq. A.14 by a parameter. This parameter then is the maximum mass and simply is also a result of the fit.

The method, however also has its disadvantages. In the case of bins, the fit has to be adapted to a number of points equal to the number of bins (in the case of the method with variable binsize, this was 84), whereas here the number of points is equal to the number of stars in the sample (in our specific example 11424). This makes the code very time consuming, especially for arrays of a large number of objects. The time the fit takes goes quadratically with the number of datapoints included.

We therefore test this method on a small part of the array of masses, ie. the first 1000 masses in the list are fitted. This list is not sorted, so this is the same as just a random sample of 1000 stellar masses. The result of the fit can be seen in Fig. A.4. The fit agrees reasonably well with with the data as well as with the expected Salpeter value of -2.35. The error on the slope is much bigger than in the previous fit methods. That is the result of the fact that there are only 1000 out of 11424 stars taken into account.

The conclusion can be made that this method of fitting is fairly good, but has the big disadvantage of not being able to handle a large amount of data, like probably necessary for the project of this thesis.

Maximum likelihood fitting

In the last method I review here we make use of the probability density function again (i.e. the distribution function normalized, such that the total integral equals unity). The method is explained in detail in e.g Bevington & Robinson (2003) and therefore I will only briefly discuss it here.

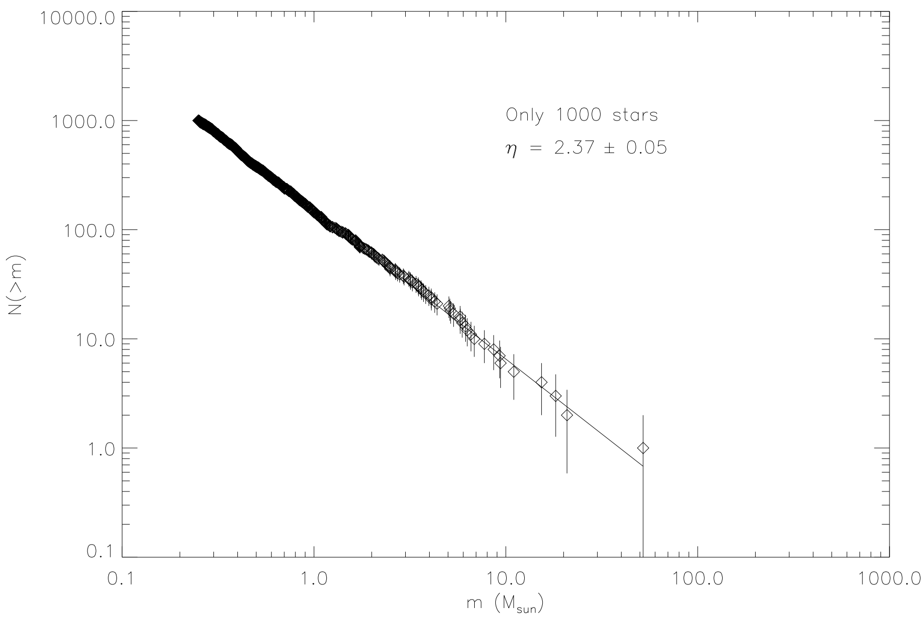

Figure A.4:
The result of a fit using the cumulative mass spectrum. The data are plotted according to Eq. A.14 and a power law fit to 1000 stars from the sample used before. The errorbars are 'poissonian' in the sense that they are just the square root of the value on the vertical axis, which is the number. This represents the fact we estimate them to be on the median of their own probability interval.

The idea is to maximize the likelihood that certain values of the parameters to be fitted are the right values, followed by a comparison with other values. The most probable value then is taken to be the result of the fit. For a PLDF the likelihood function (LF) is created in a very easy way:

$$LF = \prod_i f_i \tag{A.15}$$

$$f_i = \text{PDF}(x_i) = C \cdot x_i^{-\alpha} \tag{A.16}$$

The right hand side of this equation represents the PDF , just like in Eq. A.5: x_i are all data points, $-\alpha$ is the slope of the powerlaw and C is the normalization constant, taken such that the total integral over the DF will equal unity.

Because the numbers involved (the probability density at the data points) are usually very small (and they are even multiplied), usually the logarithm of the likelihood function is used:

$$\log LF = \sum_i \log f(x_i) \tag{A.17}$$

Ofcourse, maximizing this logarithm is the same as maximizing the likelihood function itself.

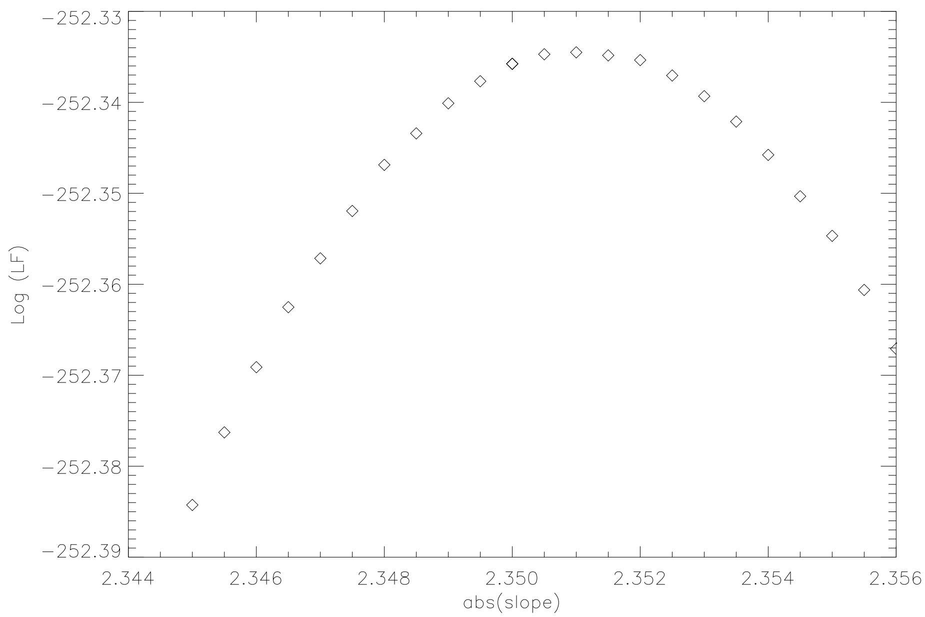

Figure A.5:
The logarithm of the likelihood function as a function of the trial slope. Note the extremely small values on the vertical axis.

In practice one makes an (educated) guess of the outcome of the fit and then perturbs it in both directions to finally become a best fit result. Here, one can see that the precision of this method stands with the stepsize one takes for the perturbations of the parameters to be fitted. Especially when fitting several parameters this involves large calculations (number of datapoints times number of values for the first parameter times number of values for the second and so on ...) and therefore one cannot take the steps ever smaller. The precision is therefore linked to the stepsize you take.

The likelihood will only give the slope of the powerlaw, as the normalisation is determined by the datapoints and the slope you try in a specific calculation of the likelihood function. In the end you are able to determine the 'real' normalisation, using your best-fit slope and the total number of datapoints. How the likelihood varies with the guessed slope can be seen in Fig. A.5.

What about the standard deviation of the fit method? The most easy way (and the most general one as well) is one in which you perform Monte Carlo simulations of artificial datasets with the same number of points, distributed according to your best-fit distribution function. The slopes fitted back will give a Gaussian distribution (centered around the slope you put in, in an ideal case) of which the 1σ value is the 1σ value of the fit. This gives an independent way of obtaining the standard deviation of the fit and it will solely depend on the number of datapoints.

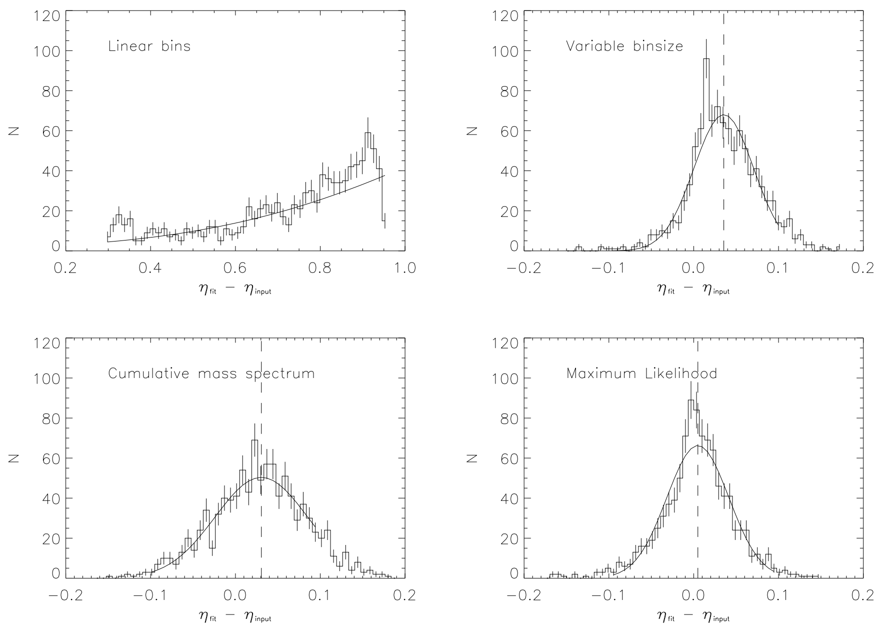

Figure A.6:

For the fit methods described in the previous section we plot here the differences between the fitted slope and the input slope. The absolute value of the slope is taken here, so the slope of a Salpeter mass function is 2.35 in this case. A best fit Gaussian is overplotted. Of particular importance is the place of the peak of this Gaussian, which would ideally be zero. Big differences between the methods are seen and discussed in the text. The vertical dashed lines are the places of the peaks of the fitted Gaussians. Note also that the scale of the horizontal axis is different for the upper left panel.

A.3.4 Comparing the results

In the previous sections we just gave a fitresult of a fit to one particular array. This already gives insight in the goodness of the fit, but a more quantitative comparison can be made. In order to do so we repeat the process of random sampling 1000 times. Every time we fit the array using our different fit methods. Every time we record the slope of all four the methods, in order to get a distribution of fitted slopes, where the input slope always is the same. Of course the fit results in a slope and an error on the slope. The method therefore already 'admits' to be a bit wrong. To get a useful way of comparing the methods, we will look at the distrubtion of $(\eta_{\rm fit} - \eta_{\rm input})$. In principle, one should divide this quantity by the standard deviation of the fit. The expectation is that we find a more or less Gaussian distribution of fit offsets. The best fitting method of course gives a Gaussian with a peak as close as possible to 0 and a width of 1. I will not do so here, because the maximum likelihood method will give you a standard deviation that is derived from Monte Carlo simulations, so the peak of this gaussian will by default be of width 1. Therefore the comparison will be a bit unfair (we can then only judge on the place of the peak, which will have to be close to zero anyway.

To come again a bit closer to reality, these 1000 clusters will not have the same mass, nor the same number of stars, but rather masses distributed according to a power law mass function, with a slope of -2 (see eg. Zhang & Fall (1999); de Grijs et al. (2003c)) and a minimum cluster mass of 100 $M_{\odot}$. The total number of stars that have to be drawn from the DF is calculated using Eq. A.2. The sum of all these masses will probably not be exactly equal to the previously sampled cluster mass, but this effect will easily average out over 1000 clusters.

The method of the cumulative mass spectrum is only able to handle datasets with a 1000 elements maximum within a reasonable time. Therefore, when creating a larger array of stars, only the first 1000 are used in this fit method. The other methods will all fit on all the data.

For every series of fitting we will use the same array of stellar masses. In other words, when an array of masses is created, this particular array will be fitted with all four methods, to have an honest comparison. This opposite to the easier method in which you just seperately test all the four methods on their own.

The results can be seen in Fig. A.6. For all four methods the offset in the fitted slope with respect to the input slope is fitted with a Gaussian. The first feature that strikes the eye is the upper left panel (equally spaced linear bins), and its very non-Gaussian distribution of offsets. It is clear that this method really messes up your data. The fact that one does not see anything like a Gaussian is mainly caused by the very sensitive dependence of the goodness of the fit to the number of points fitted (actually: to the number of points in the bins). In any case, the slope fitted back is too shallow.

The method using the cumulative mass spectrum gives Gaussian distributed slopes, centred at 0.03, fairly close to zero. The big disadvantage of throwing away every datapoint but the first 1000, makes the method less precise and desirable (who wants to throw away data?) and therefore it will not be used in the investigations in this thesis.

The method with variable binsizes (and in every bin approximately the same number of datapoints, differing by at most one) is also doing fairly well. The offset has a mean of less than 0.05. The width of the gaussian should be comparable to a typical standard deviation of a fit. Although this method does a good job (it even has an extra peak, very close to zero), the last one will be even better, as will become clear.

The maximum likelihood method has the sharpest peak, the closest to zero: within 0.01. The precision of the fit will in the end be determined from Monte Carlo simulations of the kind presented here, in which the standard deviation of the fitted slopes will be taken as the standard deviation of the fit method. Therefore the precision will be determined every time in a statistically independent way and so will be trustworthy.

The method of maximum likelihood is the method that will be used to fit power law distribution functions whenever needed throughout this thesis (unless stated otherwise).

A.4 Double power law distribution functions

Luminosity functions of star clusters are often not well described by single power laws, but they rather resemble a double power law distribution (two distinct power laws, divided by a bend at a certain magnitude), see e.g. Whitmore et al. (1999); Gieles et al. (2006b,c). When fitting such a distribution using the maximum likelihood method now consist of simultaneously fitting three quantities (or four if you also want to fit on the normalization): two slopes and a bend position. The likelihood function therefore now is a function of at least three variables, resulting in the possible existence of multiple (local) minima. Besides that, the computational time now, for the same precision as a single powerlaw fit, will have to be cubed.

By testing the method in ways similar to the ones described before (random sampling of a DF and fitting back the input values) I found out that the end result also is very sensitive to initial guesses and fitting boundaries. I have therefore chosen to fit double power law distribution functions with the method of equally high bins, described in section A.3.2; which was the best method using bins. The other method without bins is usually too slow for the number of data this thesis deals with.

Appendix B

Summary for non-astronomers

In this appendix I will try to explain in somehwat easier terms what I did during the last year of my Masters program. I hope to be able to explain to people without training in physics or astronomy what I did, why I did it and what the results are. Although this appendix is meant for non-specialists I do expect the reader to have some basic knowledge about physics and astronomy. The terms star and galaxy should ring a bell, as well as the words gravity and tidal force (just to mention a few examples). Be aware of the fact that this is a *summary* for the layman, so I will not describe every single detail that matters in this research.

The structure of this summary will be comparable to the structure of the rest of this thesis. I will also refer to figures in the rest of this thesis in order not get them in all double. I will start with a brief description of star clusters and explain their properties. The introduction is somewhat more elaborate than the normal text, because of the lack of knowledge that is to be expected from non-astronomers. I will shortly compare the clusters in our Milky Way Galaxy with cluster populations in other galaxies (and the differences in research carried out). After a short discussion of what clusters do when they are in interaction with their environment I will explain the central question of this thesis: is there any relation between cluster properties and the location of the cluster in its host galaxy? I will then end with the results (skipping most of the details about the method) and a short outlook on what can be done in the near future.

B.1 Star clusters in different galaxies

In the universe, a whole hierarchy of structures can be recognized. Starting from the bottom, we have the stars, which for a lrage fraction do not stand alone, but rather form binaries or multipole stars: they 'belong' to each other and orbit one another due to their mutual gravitation. Especially young stars, but also some of the older ones, group also in larger agglomerations, star clusters. Two examples of clusters (an old one and a young one) are shown in Fig. 1.1 and 1.2. These clusters, together with the stars that do not belong to a cluster, the *field stars*, group together in galaxies, of which an example can be seen in

Fig. 3.2, and more will follow in a section below. These galaxies in turn form groups, called clusters of galaxies. In the rest of the text, wherever I just write 'cluster', I mean *star* cluster and not a cluster of galaxies. On the largest scale, clusters are located along a foamy structure, with huge, almost completeley empty 'bubbles' in between.

This thesis is about clusters, the largest structures we are concerned with are galaxies. In this section I will provide the necessary background about star clusters and galaxies.

B.1.1 Star clusters

A star cluster is a so-called simple stellar population. This basically means that they were born together at the same time. All stars in a cluster are therefore of equal age and initial composition (this composition changes in the center of a star due to nuclear fusion). They consist typically of several hundreds up to a few (tens of) million stars.

The stars move around on rather chaotic trajectories under the influence of the gravitational forces of all other stars. The evolution of a cluster is therefore governed by two kinds of evolution: dynamical (due to the gravitational and tidal interactions) and stellar evolution (every star on itself goes through the evolutionary phases, as if it were a single star). Sometimes these effects mix up (e.g after the merger, or very close interaction of two stars), complicating the detailed cluster evolution. Both these kinds of evolution will be explained in somewhat more detail below.

B.1.2 A diversity of galaxies

These clusters reside in their host galaxy, and the surroundings of a cluster have a large impact on the dynamical evolution of these objects. It is therefore important to know what the differences are among these morphological types of galaxies. I will only describe the morphological types here; details on e.g. origin and evolution are to be found elsewhere.

In this description I will make use of the so-called Hubble tuning fork, a schematic overview of the different morphological types, originally put forward by Edwin Hubble (Fig. B.1). The left part of this diagram contains the elliptical galaxies. These are in general quite red and massive. They contain hardly any gas and dust and therefore they are currently not forming stars anymore. They are slowly evolving because of the stellar evolution.

The other side of the fork (the fork part) contains the, usually younger, normal and barred spirals. These flat, disk-like galaxies (in Fig. B.1 they are imaged face on) have a large content of gas and dust and use this to form stars. The galaxy under investigation here is an Sc type galaxy, as can be seen by comparsion if Figs. B.1 and 3.2. Young cluster populations can of course only exist in star forming galaxies, so the ellipticals will only contain old clusters. Because clusters die rather young, usually, it is best to look at spirals in order to investigate the dynamical evolution of star clusters (spirals also contain some, typically in the order of a few hundred, old clusters).

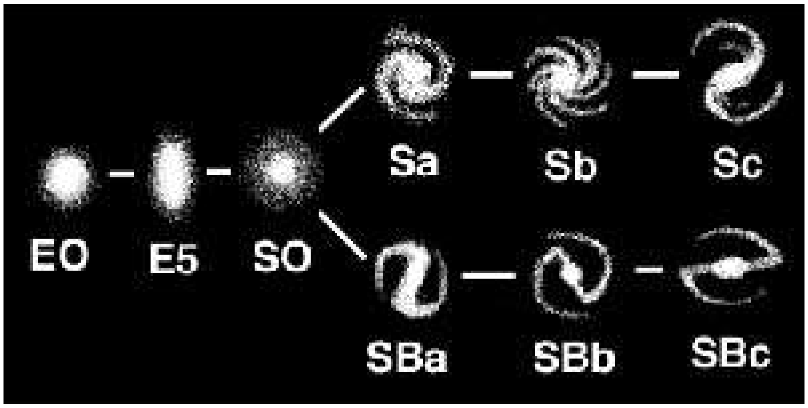

Figure B.1:
The morphological classification of galaxies by Edwin Hubble. On the left one sees the elliptical galaxies (usually old, red and massive). On the right we have the normal spirals (upper half) and barred spirals (lower half). Spirals are generally younger and have a huge content of gas and dust.

B.1.3 Galactic vs. extragalactic cluster research

The main difference between clusters in our Milky Way Galaxy (galactic clusters) and the ones in other galaxies (extragalactic clusters) is of course their distance. Extragalactic clusters are very much further away, and therefore appear to our telescopes much fainter and smaller. Galactic clusters are usually totally resolved, meaning that we can see all the stars separately as more or less point sources. Extragalactic clusters are so far away that we can only see the total light of all its stars together in a source that is just slightly bigger than a point source (i.e. a bright dot, containing the light of all stars in the cluster).

It therefore is a greatly different kind of research when analyzing extragalactic clusters as opposed to galactic clusters. The way in which one analyzes galactic clusters is of no importance for this thesis, and therefore I will only briefly describe what the basic idea is of the analysis of extragalactic clusters.

The fact that we see only the light of all stars together makes life a lot harder. If you don't know the age and mass of the cluster, you in principle don't know what kind of stars are in there. An additional problem is that the light from the cluster travels through clouds of gas and dust on its way here, making the light dimmer and redder. The challenge now is to see how you can create the spectrum of light (distribution of the intensity with wavelength or color) you receive from the clusters by chosing an appropriate cluster mass, age and extinction (the reddening and diminishing effect of gas and dust).

Integrating star light of clusters

From theories of stellar evolution we know the spectrum of the light emitted by stars of all different masses and all different ages. In principle it is straightforward to take an arbitrary mass, and add all this spectra up (for the same ages, because clusters are single aged) and see if this looks like the light that we receive from the cluster. If not, take a different mass and try again. In this way you can fit the age, mass and extinction of every cluster separately.

Unfortunately, this is not as easy as it may seem. In the first place, obtaining spectra of all clusters is an observation time consuming operation. Therefore we take a very rough measure of it, called the spectral enery distribution (SED). This basically is a spectrum, but with a very low resolution (only measuring the intensity of the light in a very restricted number of wavelength intervals, whereas a full spectrum has a measure of the intensity at very many different wavelengths). In this way one looses a bit of information, but general information on the color of the clusters is still available, and that is the main source of information.

A cluster is born with all kind of stellar masses. Most of the stars are of low mass, very few are very massive. This distribution over different masses is more or less constant from cluster to cluster. Therefore, if one knows the total mass of the cluster, one can predict which stars are in it (the relative numbers of different masses are known, and the sum of all masses is the cluster mass). For all of these stars the evolution is known in quite some detail as well. Most of the stars hardly change their appearance for about 90% of their total lifetime. This total lifetime depends on the mass; the more massive a star is, the less its total lifetime will be. A star like the Sun will live for 10 billion years, the most massive stars already die at an age of 10 million years.

Whenever a star dies, it stops shining and they therefore only contribute to the light of the cluster during their life, most of which is in a very quiet phase, without major changes. In the last 10% it is also known what the starlight does (basically it gets brighter and very red (so called red giant stars)). The older the cluster becomes the less stars contribute to their total light, with the maximum stellar mass that is still in getting lower and lower. Clusters therefore get less and less bright as they age. Moreover, less massive stars are redder, and so the cluster gets redder and redder with the years.

A combination of the color of the cluster and the brightness gives you an indication of the age and mass of the cluster. The color is not so much depenedent on the mass, so from the color you can determine its age. Knowing this age and the brightness then gives you the clusters mass.

Problems in analyzing clusters

This all sounds easy and straightforward to do. There are, however, some serious problems to solve. All these problems have to do with so-called degeneracies. This basically means that several different processes have the same effect on the light we receive from a cluster, and that is therefore hard to distinguish one from the other. Clusters get redder and fainter when they age. If the light of a cluster moves through a dusty cloud on its way here, it gets fainter and redder (scattering of the light out of the line of sight is more important for blue light) as well. The chance that the light moves through a cloud is not at all small: clusters are born in the cold cores of clouds, so they are most likely embedded in the remainders of their parental clouds. An extra side effect is that the original composition of the stars in the cluster (which basically is the composition of their outer layers, which are emitting the light you see) also affect their color. So, whenever you don't know the composition of the stars, and the amount of extinction (light 'absorption' by clouds in between), it is very hard to determine the age and mass of the cluster.

Several people in the world have come up with methods to make a difference between the effects. The one being more succesful than the other, all methods *do* need measurements of he brightness of the clusters through multiple filters, in wavelengths ranging from the near UV to the near IR. Whenever these observations are not at hand, it is not possible to unravel extinction, mass, age and metallicity reliably and one has to rely on other methods.

The luminosity function of a cluster population

One such methods is the luminosity function. Although it is not the easiest tool to grasp, I will explain it here, because an important part of my research made use of it.

A luminosity function is a so-called distribution function (those of the readers, who do not know what that is and are not afraid of mathematics, may try Appendix A). This means that for every value of a luminosity, the luminosity function gives you a measure of the chance that a randomly chosen luminosity has that particular value. Examples of luminosity functions (LFs) can be seen in Fig. 6.1 through 6.4.

Models of star cluster populations, also called synthetic cluster populations, can be created with the help of computers. These are models in which one makes assumptions on the distributions of masses and ages of all clusters in the population. The age and mass of a cluster together give their luminosity in different passbands (filters). Putting all these luminosities together results in the distribution of luminosities, i.e. the luminosity function. Changing parameters in the original input (age and mass distribution) results in different LFs. Besides observing an LF, one can adapt the input of the synthetic population, to *model* the LF and compare observations and models.

One thing that can be found in this way is that, if there exists a physical upper mass limit to star clusters, this will show up as a bend in the LF, like can be seen in Fig. 6.1 through 6.4. The location of this bend tells you something about the value of this maximum mass: the brighter it is, the more massive clusters are.

B.2 Evolution of star clusters

Cluster are not at all steady objects. They are subject to the evolution of their constituents stars and are in continuous dynamical evolution. In this section I will explain why they evolve and how they evolve.

B.2.1 Cluster dynamics

Ignoring the first ten million years of their existence (which are complicated and fall outside the scope of this thesis), stellar evolution is not very important for the dynamics of star clusters. This nevertheless doesn't mean that clusters don't evolve during the remaining time.

Stars in a cluster constantly attract each other gravitationally. It is therefore necessary that they have sufficiently high speeds, in order not to collapse towards the center (basically the same effect as the earth in its orbit around the sun: if it would move faster it would move away from the sun, whereas it would move towards the sun if it went slower in its orbit). All stellar motions are more or less random in the gravitational field of the cluster; they do not all move on beautiful circular orbits around the center.

Isolated star clusters

Let's first consider a star cluster that is on its own in the universe: no galaxy where it moves in, no neighbouring clusters or any other massive objects like giant clouds of gas and dust. In such a cluster, stars are solely under the influence of the gravity of all other stars in the cluster. In principle a star moves as a result of all the other attracting stars, without noticing that the net force it experiences actually *is* the result of gravitional forces of all other stars. Every now and then (quite often in a dense cluster), stars come rather close to each other. In an interaction between two stars they tend to exchange energy in such a way that their energies come closer to each other. In practice this will mean that a massive star slows down, while the less massive star will speed up. The slower star will sink to the center of the cluster, while the faster star is able to move further out. If a star is in the outer parts of a cluster and gets another 'kick' it might move fast enough to leave the cluster forever (i.e. it moves with a velocity bigger than the escape velocity), leaving the cluster behind with one (not too massive) star less. The core, on the other hand, will get populated with more and more (on average quite massive) stars with an ever increasing concentration.

The cluster gets less and less massive due to the 'evaporation' of stars from the outside. These stars are the stars that make up the field star population as we observe it today. The core of the clusters is getting denser and denser. In principle this will lead to the collapse of all of these stars onto each other, but this is overcome by the formation of binary systems. Stars 'capture' each other, which releases energy. That energy is used to let the core expand a bit again. So a cluster on its own will, in due time, get a concentrated core and an ever expanding (although slower and slower expanding) envelope.

This is not the only cluster disrupting process. The fact that cluster do not live alone in the universe makes their dynamical evolution more interesting, more complicated and faster (i.e. leading to total disruption in less time). All other dynamic processes (which I will describe below) lead to so-called 'heating' of the cluster. This means that the stars get higher random velocities, in which of course a part of the stars will get a velocity higher that the escape velocity, and as such accelerate the evaporation of the system.

Tidal interaction

A first interaction mechanism is tidal in nature. If stars are in the outskirts of the cluster, for example at the side of the center of the galaxy the cluster belongs to, it might get in a region where the forces due the gravitational field of the galaxy are stronger than the gravitational attraction of (all the other stars in) the cluster. This star will move, now, under the main influence of the host galaxy instead of the cluster. Because it is closer to the center of the galaxy than the cluster is, it moves on an orbit with higher velocity, and therefore it will speed up in front of the cluster. This star is lost. If the star, on the other hand, is at the back end of the cluster, it should (according to the gravitational field of the galaxy) move on a *slower* orbit. So, if it is far enough from the clusters center (in order to be more or less equally influenced by the cluster as by the galaxy), it will lack behind and also be lost from the cluster. This effect is clearly illustrated by the extreme example of Pal 5, Fig. 1.3.

Shocks

For clusters in a spiral galaxy, clusters can get shocked as well. If we are concerned with a cluster on an orbit which moves through the disk twice in its orbit, this is called disk shocking, whereas for cluster on an orbit in the disk of the galaxy (usually the young clusters) it is called arm-shocking, because when revolving around the galaxy center it will pass through spiral arms. Why are clusters shocked at these locations? I will only describe it here in terms of arm shocking (for most of our clusters are in the disk), but the same will hold for clusters in the halo of a galaxy, when moving through the disk.

Coming in the vicinity of a spiral arm, which basicaly is just a region of higher density, a cluster starts to experience a bit more gravitational attraction towards this spiral arm. The front end of the cluster will notice this effect a bit earlier than the rear end and will therefore be accelerated the first. This will stretch the cluster. Once 'inside' the spiral arm the stars of the cluster will have to make some effort to move out again, so then it decelerates, whereas the back end of the cluster is still coming in at high speed. This squeezes the cluster a bit. Moving out as a whole brings a cluster more or less back to its original proportions (in size, *not* in mass). While being stretched and squeezed it may have lost a considerable amount of stars, sometimes even up to 25%!

B.2.2 What do we want to know?

Although the outline of cluster evolution is more or less fixed, a lot of details are still unknown. This thesis touches upon two of these details, with one common factor. We will use observations of the disk galaxy M51, as can be seen in Fig. 3.1 of which a composit is shown in Fig. 3.2, to touch upon the following questions:

1. What is the distribution of **radii** of star clusters in M51? In particular: is this distribution of radii different for different subsets, if we create these subsets on a basis of position in the disk of the galaxy? For these different subsets one can think of:
   (a) Close to the center of the galaxy or further to the outskirts
   (b) Inside the spiral arms or in between the spiral arms
2. What is the distribution of luminosities? This distribution is also called the **luminosity function**. Here, the same subsets are created as mentioned with respect to the radii.

In the rest of this summary I will describe the results, without going into the details of data reduction.

B.3 Radii of star clusters in M51

B.3.1 Observations

In order to measure the radii, first all the clusters have to be identified on the image. Point sources are selected and a dedicated software package is used to measure the size of the object. It turned out that obtaining *reliable* size determinations were not that easily extracted from the image. Conclusions on the distribution of radii are as yet not 100% definitive. General statements on the distribution are not expected to be very much off, but the details may change in due time.

B.3.2 Results

The distribution of radii can be seen in Fig. 5.1. The horizontal axis in this case is logarithmic, with the tickmarks indicating the normal, linear, scale in steps of 1 parsec (= pc, =3.26 lightyears, $=3 \cdot 10^{18}$ cm). The shape of the distribution is somewhat unusual. The part right of the peak looks pretty much like shapes people found before. Left of the peak is a part which previous extragalactic studies couldn't reach, because the resolution was insufficient.

The distribution is peaked at around 3 pc. This seems to be a sort of preferred radius. Also in other galaxies, like our own Milky Way Galaxy, radius distributions are peaked around more or less this value.

The question whether or not this distribution depends on galactocentric distance is adressed in Fig. 5.2. Here the red squares are the mean radius at that particular, indicated distance. The dashed line is a fit through the data points. The solid lines is the line which fits the radii of the old, globular cluster system of our Milky Way system. The dashed-dotted line is the line that describes an equilibrium between the star cluster and the tidal field of the galaxy: If star clusters have a radius such that it is *just* not being torn apart by the tidal forces of the galaxy, then the radii are increasing according to that line for clusters further out.

The two lines, of which one corresponds to a largely young population (our M51 clusters) and one to an old cluster population (the globular clusters), might indicate a very slow evolution towards tidal equilibrium. The young system is 'born' with more or less random radii (with a distribution peaked at around 3 pc), and they are evolving towards an equilibrium. The old system is therefore already much closer to this equilibrium, but still not quite there.

A relation with background intensity (so basically being in- or outside a spiral arm) is not found.

B.4 Luminosities of star clusters in M51

B.4.1 Observations

In order to say something about the luminosity of clusters we have to select point sources that are really clusters (so to *remove* the stars that are in the image from the list of point sources) and to measure the amount of light that comes from them. This amount of light has to be corrected for absorption along the way (it moves through clouds of gas and dust) to know the intrinsic amount of light emitted, i.e. the luminosity.

B.4.2 Results

Once this is done, we can create the luminosity function. In the three different filters they look like Fig. 6.1 through 6.3 in the upper panels. On the horizontal axis you see the absolute magnitude, which is an astronomical measure of the amount of light they emit. Left means dim, right means bright, and a shift of a certain number in magnitudes corresponds to a *factor* difference in luminosity (so it is a logarithmic scale as well): 5 magnitudes brighter means a factor 100 brighter.

The most important result is the fact that we significantly detect a bend in this function, indicated by the vertical dashed line. As mentioned before this means that there is a physical upper mass limit for star clusters in M51. We detect the bend in all three filters, so that strengthens the claim.

B.4.3 Maximum mass at different loci

The lower panels of the LF plots show the luminosity functions of several subsets of the population, with their galactocentric distance as parameter. The upper of the three is the population closest to the center, going further out for the lower plots. We can see here that the bend occurs at brighter magnitudes, closer to the center of the galaxy, indicating that the mass truncation lies at higher masses in the center of the galaxy.

In Fig. 6.4 the luminosity function is shown as a function of 'region'. High and low background regions are selected, as shown in Fig. 4.1. The intermediate region is discarded, because there were too little clusters to have reliable statistics; it is only used as a clear distinction between the other two regions. From this LF it is clear that there is some sort of a difference in bend location, although it is less significant than in the case of the galactocentric distance requirement.

B.4.4 Cluster disruption

From the slope of the faint (i.e. left) side of the LF we can also say something about the rate at which clusters are destroyed. This slopes results from the distribution of initial masses of the clusters and from the disruption of the clusters in due time. A shallower slope means faster disruption. We can conclude therefore that cluster are faster disrupted in the center of the galaxy and in regions of higher background intensity.

In summary, the results of an investigation of relations between LF parameters and location are:

1. The bend in the LF occurs at *brighter* magnitudes, *closer* to the center of the galaxy

2. The location of the bend in the LF is largely *independent* of background intensity

3. The slope of the faint end side of the LF is *shallower, closer* to the center of the galaxy

4. The slope of the faint end side of the LF is *shallower* in *high* background regions

B.5 Conclusions and outlook

The radius distribution seems to be peaked at a value of around 3 pc, decreasing fast towards larger as well as smaller radii. Any relation between mean radius and postion in the galactic disk is *not* found, implying that the comparatively young cluster population is *not* (yet) in tidal equilibrium with their host galaxy (old globular clusters in our Milky Way halo are much closer to this equilibrium).

Using the LF of the star cluster population of M51 we show that the cluster initial mass function is likely to be *truncated at the high mass end*. We also show that the maximum possible cluster mass in the central regions of the galaxy is higher than in the outskirts. Regions of higher background intensity also tend to form more massive clusters.

Slopes of the luminosity function indicate a more efficient cluster disruption process in the inner parts of the galaxy than in the outer parts, and more efficient disruption in high background regions than in regions with lower background intensity.

Of course the work is not done here. Although being a step further in understanding the formation and evolutionary processes that a star cluster goes through, lots of questions are still unanswered, or only partially answered. For example the question of the maximum mass: why is it there? In which other galaxies can we see it? How do these other galaxies compare to M51? Are there galactic systems (like e.g. merging galaxies) where such an upper mass limit does not exist? What about the old systems, which were formed under very different circumstances than the young system we observed? And many, many more...

Also in the area of cluster radii a lot of work is still to be done. Not only will observations learn us more about the complicated dynamical evolution of many stars, also simulations will grow more and more realistic in due time. The final words are not yet spoken.

Bibliography

Anders, P. & Fritze-v. Alvensleben, U. 2003, **A&A**, 401, 1063

Bastian, N., Gieles, M., Efremov, Y. N., & Lamers, H. J. G. L. M. 2005a, **A&A**, 443, 79

Bastian, N., Gieles, M., Lamers, H. J. G. L. M., Scheepmaker, R. A., & de Grijs, R. 2005b, **A&A**, 431, 905

Baumgardt, H. & Makino, J. 2003, **MNRAS**, 340, 227

Bertelli, G., Bressan, A., Chiosi, C., Fagotto, F., & Nasi, E. 1994, **A&AS**, 106, 275

Bertin, E. & Arnouts, S. 1996, **A&AS**, 117, 393

Bevington, P. R. & Robinson, D. K. 2003, Data Reduction and Error Analysis for the Physical Sciences (McGraw-Hill)

Bik, A., Lamers, H. J. G. L. M., Bastian, N., Panagia, N., & Romaniello, M. 2003, **A&A**, 397, 473

Binney, J. & Tremaine, S. 1987, Galactic dynamics (Princeton, NJ, Princeton University Press, 1987, 747 p.)

Boily, C. M. & Kroupa, P. 2003, **MNRAS**, 338, 673

Boutloukos, S. G. & Lamers, H. J. G. L. M. 2003, **MNRAS**, 338, 717

D'Agostino, R. B. & Stephens, M. A. 1986, Goodness-of-fit Techniques (New York: Marcel Dekker)

de Grijs, R., Anders, P., Bastian, N., et al. 2003a, **MNRAS**, 343, 1285

de Grijs, R., Anders, P., Lamers, H. J. G. L. M., et al. 2005, **MNRAS**, 359, 874

de Grijs, R., Bastian, N., & Lamers, H. J. G. L. M. 2003b, **MNRAS**, 340, 197

de Grijs, R., Fritze-v. Alvensleben, U., Anders, P., et al. 2003c, **MNRAS**, 342, 259

Einstein, A. 1921, Festschrift der Kaiser-Wlhelm Gesellschaft zur Förderung der Wissenschaften zu ihrem zehnjärigen Jubiläum dargebracht von Ihren Instituten (Springer, Berlin, p. 50)

Elmegreen, B. G. 2002, **ApJ**, 577, 206

Elmegreen, B. G. & Elmegreen, D. M. 2001, **AJ**, 121, 1507

Elson, R. A. W., Fall, S. M., & Freeman, K. C. 1987, **ApJ**, 323, 54

Fall, S. M., Chandar, R., & Whitmore, B. C. 2005, **ApJL**, 631, L133

Feldmeier, J. J., Ciardullo, R., & Jacoby, G. H. 1997, **ApJ**, 479, 231

Fellhauer, M. & Kroupa, P. 2005, **ApJ**, 630, 879

Fruchter, A. S. & Hook, R. N. 2002, **PASP**, 114, 144

Geyer, M. P. & Burkert, A. 2001, **MNRAS**, 323, 988

Gieles, M., Athanassoula, E., & Portegies Zwart, S. 2006a, **A&A**, in prep.

Gieles, M., Bastian, N., Lamers, H. J. G. L. M., & Mout, J. N. 2005, **A&A**, 441, 949

Gieles, M., Larsen, S. S., Anders, P., Bastian, N., & Stein, I. T. 2006b, **A&A**, 450, 129

Gieles, M., Larsen, S. S., Scheepmaker, R. A., et al. 2006c, **A&A**, 446, L9

Gieles, M., Portegies Zwart, S., Sipior, M., et al. 2006d, **A&A**, in prep.

Girardi, L., Bressan, A., Bertelli, G., & Chiosi, C. 2000, **A&AS**, 141, 371

Goodwin, S. P. 1997, **MNRAS**, 284, 785

Haas, M. R., Gieles, M., Scheepmaker, R. A., et al. 2006, **A&A**, in prep.

Harris, W. E. 1996, **AJ**, 112, 1487

Harris, W. E. 2001, in Saas-Fee Advanced Course 28: Star Clusters, ed. L. Labhardt & B. Binggeli, 223–+

Heggie, D. & Hut, P. 2003, The Gravitational Million-Body Problem: A Multidisciplinary Approach to Star Cluster Dynamics (Cambridge University Press, 2003, 372 pp.)

Henon, M. 1973, in Saas-Fee Advanced Course 3: Dynamical Structure and Evolution of Stellar Systems, ed. G. Contopoulos, M. Henon, & D. Lynden-Bell, 183–+

Hunter, D. A., Elmegreen, B. G., Dupuy, T. J., & Mortonson, M. 2003, **AJ**, 126, 1836

Jordán, A., Côté, P., Blakeslee, J. P., et al. 2005, **ApJ**, 634, 1002

Kharchenko, N. V., Piskunov, A. E., Röser, S., Schilbach, E., & Scholz, R.-D. 2005, **A&A**, 438, 1163

King, I. 1962, **AJ**, 67, 274

Krumholz, M. R. & McKee, C. F. 2005, **ApJ**, 630, 250

Lada, C. J. & Lada, E. A. 1991, in ASP Conf. Ser. 13: The Formation and Evolution of Star Clusters, 3–22

Lamers, H. J. G. L. M., Anders, P., & de Grijs, R. 2006, **A&A**, accepted, arXiv:astro-ph/0601606

Lamers, H. J. G. L. M., Gieles, M., Bastian, N., et al. 2005, **A&A**, 441, 117

Larsen, S. S. 1999, **A&AS**, 139, 393

Larsen, S. S. 2002, **AJ**, 124, 1393

Larsen, S. S. 2004, arXiv:astro-ph/0408201

Larsen, S. S. 2004, **A&A**, 416, 537

Lee, M. G., Chandar, R., & Whitmore, B. C. 2005, **AJ**, 130, 2128

Maíz Apellániz, J. & Úbeda, L. 2005, **ApJ**, 629, 873

Makino, J. & Funato, Y. 1993, **PASJ**, 45, 279

Melioli, C. & de Gouveia dal Pino, E. M. 2006, **A&A**, 445, L23

Moffat, A. F. J. 1969, **A&A**, 3, 455

Mutchler, M., Beckwith, S. V. W., Bond, H., et al. 2005, American Astronomical Society Meeting Abstracts, 206,

Mutchler, M., Koekemoer, A. M., & Hack, W. 2002, in The 2002 HST Calibration Workshop. Edited by Santiago Arribas, Anton Koekemoer, and Brad Whitmore. Baltimore: STScI, p. 70

Ostriker, J. P., Spitzer, L. J., & Chevalier, R. A. 1972, **ApJL**, 176, L51+

Pavlovsky et al. . 2005, ACS Data Handbook, version 4.0 (Baltmiore: STScI)

Richtler, T. 2003, LNP Vol. 635: Stellar Candles for the Extragalactic Distance Scale, 635, 281

Rosolowsky, E. 2005, **PASP**, 117, 1403

Salo, H. & Laurikainen, E. 2000, **MNRAS**, 319, 393

Salpeter, E. E. 1955, **ApJ**, 121, 161

Schechter, P. 1976, **ApJ**, 203, 297

Scheepmaker, R. A., Haas, M. R., Gieles, M., et al. 2006, **A&A**, in prep.

Schlegel, D. J., Finkbeiner, D. P., & Davis, M. 1998, **ApJ**, 500, 525

Schulz, J., Fritze-v. Alvensleben, U., Möller, C. S., & Fricke, K. J. 2002, **A&A**, 392, 1

Sirianni, M., Jee, M. J., Benítez, N., et al. 2005, **PASP**, 117, 1049

Sollima, A., Pancino, E., Ferraro, F. R., et al. 2005, **ApJ**, 634, 332

Spitzer, L. 1987, Dynamical evolution of globular clusters (Princeton, NJ, Princeton University Press, 1987, 191 p.)

Spitzer, L. J. & Chevalier, R. A. 1973, **ApJ**, 183, 565

Tremonti, C. A., Calzetti, D., Leitherer, C., & Heckman, T. M. 2001, **ApJ**, 555, 322

Tully, R. B. 1974, **ApJS**, 27, 437

van den Bergh, S., Morbey, C., & Pazder, J. 1991, **ApJ**, 375, 594

Weidner, C., Kroupa, P., & Larsen, S. S. 2004, **MNRAS**, 350, 1503

Whitmore, B. C. 2003, in A Decade of Hubble Space Telescope Science, 153–178

Whitmore, B. C., Zhang, Q., Leitherer, C., et al. 1999, **AJ**, 118, 1551

Wielen, R. 1991, in ASP Conf. Ser. 13: The Formation and Evolution of Star Clusters, 343–349

Zhang, Q. & Fall, S. M. 1999, **ApJL**, 527, L81

Acknowledgements

Without the help of many people, in very different ways, I would never have been able to complete my studies in Astrophysics with this thesis. This is the right place to thank them.

In the first place, I want to thank my parents. Their financial support made it possible for me to study Astrophysics, live in Utrecht and enjoy my spare time there. The most important thing to thank them for, though, is of course my whole life in the past 23 years and all the love they gave. My sister Femke is also to be mentioned in this respect.

Apart from them I want to thank Joyce, who managed to be my girlfriend for the past 3.5 years. I guess words are not sufficient to thank you...

During the year in which this thesis work was done, I enjoyed being a member of the $\dot{M}$-group (pronounced as M-dot, a name resulting from earlier work on stellar mass loss) and I want to thank all other members that have worked in that group in (parts of) that same year. Especially my supervisors Henny Lamers and Mark Gieles were of great importance for me in carrying out research. Also Remco Scheepmaker was always there when I had some questions.

Besides the group in which I worked there are other people to thank, like my room mates in both the rooms we were put in, class mates at several courses and general fellow students. They all made 5 years of studying fly by!

Other friends, who I am not listing here, are of course very important. I *do* want to mention the JWG, as main consumer of free hours, which without any exception were valuable and enjoyable! The other people I mean here will know for themselves. Many hours of nice chats, usually with some beer, make hard times a lot easier and fill the spare time I had with lots of fun. Thanks for all of that!